

Predicting High-Lift Aerodynamics on NASA Common Research Model - Part I: Reynolds Averaged Navier-Stokes Simulations

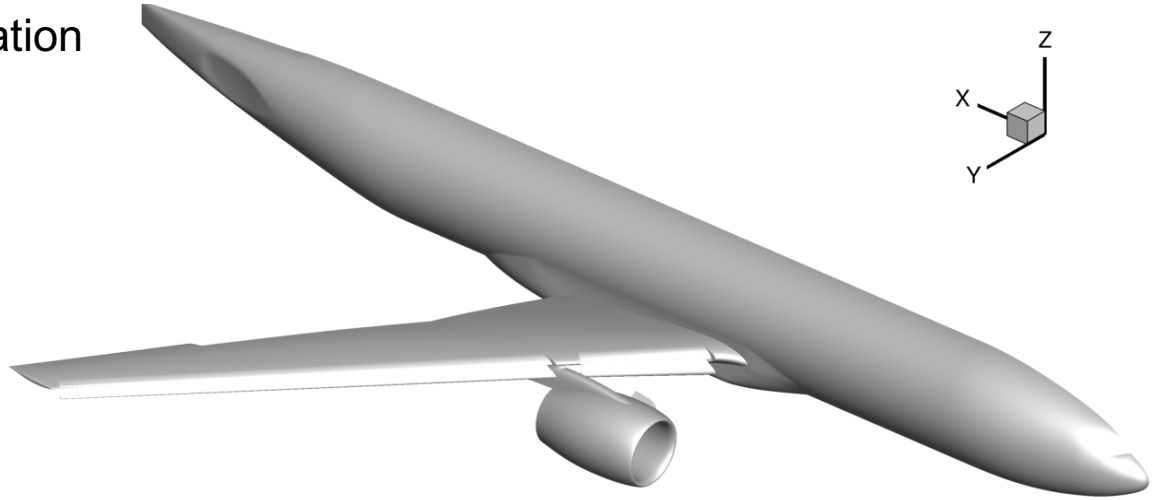
Jared C. Duensing, Jeffrey A. Housman, Luis M. Fernandes, Leonardo M. Machado, Cetin C. Kiris

NASA Ames Research Center

Advanced Modeling & Simulation (AMS) Seminar Series
NASA Ames Research Center, May 26th, 2022

Outline

- High Lift Prediction Workshop-4 (HLPW-4) Task Overview[1]
- Computational Methodology
  - Numerical methods and turbulence modeling
  - Structured overset mesh generation
- Results
  - Grid convergence study
  - Flap deflection study
  - c_{Lmax} investigation
    - Turbulence modeling
    - Alternative solution methods
    - Wind tunnel modeling
- Summary

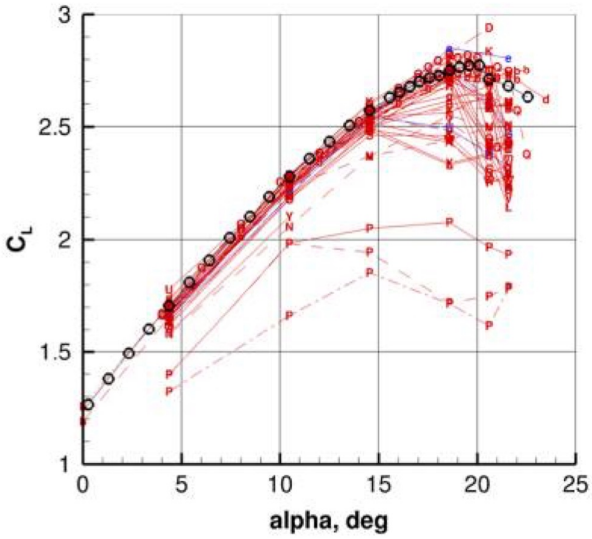


High Lift Common Research Model geometry

[1]https://hiliftpw.larc.nasa.gov/index.html

Objective

- Separated flow for high-lift configurations and high angles of attack is very challenging to predict
- HLPW-4 is organized to resolve this issue using various levels of fidelity
  - Fixed Grid RANS
  - Adaptive Grid RANS
  - High-Order Discretization
  - Hybrid RANS/LES
  - Wall-Modeled LES
- Goal: assess if RANS is sufficient to model relevant high-lift flow physics through various sensitivity studies

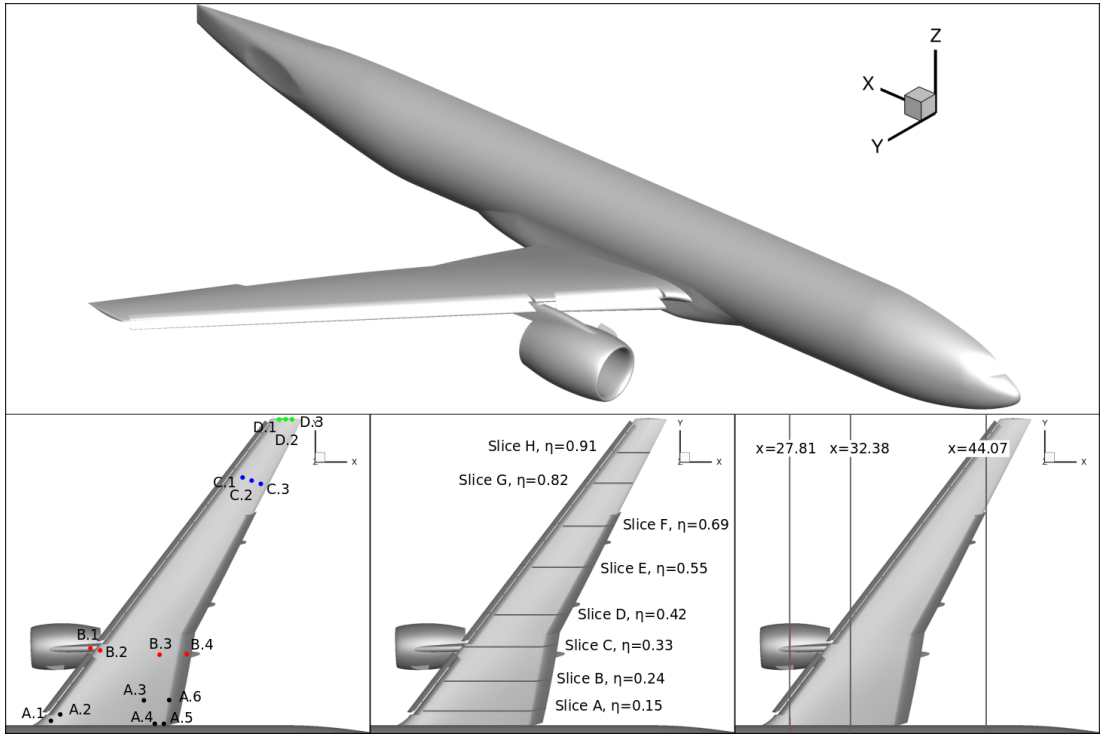


Lift predictions from the 3rd AIAA High Lift Prediction Workshop data submissions[1]

[1]Rumsey, C. L., Slotnick, J. P., and Sclafani, A. J., "Overview and Summary of the Third AIAA High Lift Prediction Workshop," Journal of Aircraft, Vol. 56, No. 2, 2019, pp. 621–644. https://doi.org/10.2514/1.C034940.

Workshop Tasks and Goals

- Use Reynolds-Averaged Navier-Stokes (RANS) methods to characterize aerodynamic performance for the High Lift Common Research Model (CRM-HL)
- Utilize workshop-provided test cases to determine RANS capability in accurately predicting complex high-lift configuration flows
- Determine best-practice modeling techniques using various studies to maximize RANS predictive capability
  - Grid sensitivity study
  - Turbulence model sensitivity study
  - Wind tunnel modeling study

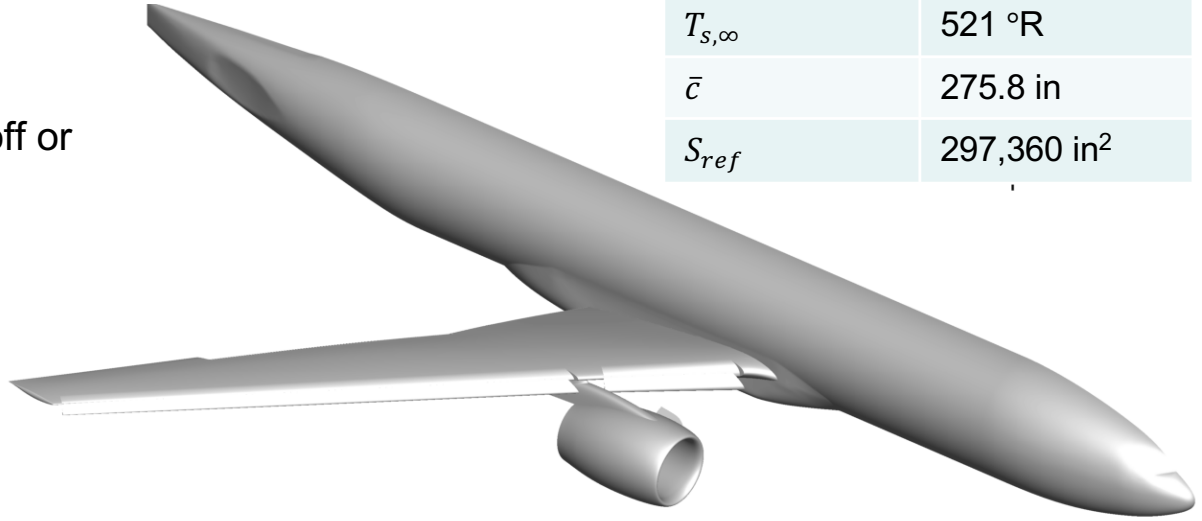


Extraction locations for various quantities including velocity (left), pressure (center), and vorticity (right) profiles

CRM-HL Geometry Overview

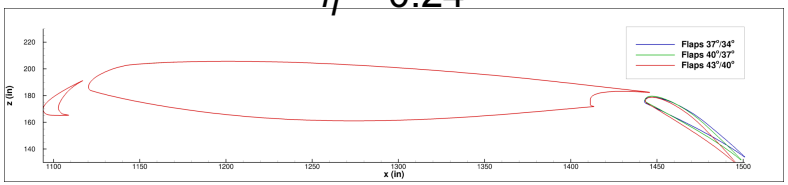
- The CRM-HL represents a high-lift aircraft configuration that embodies designs commonly found in modern commercial aircraft[1]
- Full-scale geometry provided by the committee would be used for CFD simulation
- High-lift devices are deployed to realistic deflection angles characteristic of a takeoff or landing scenario

Quantity	Value
$Mach$	0.2
Re_{MAC}	5.49 M
$T_{s,\infty}$	521 °R
$\bar{c}$	275.8 in
S_{ref}	297,360 in^2

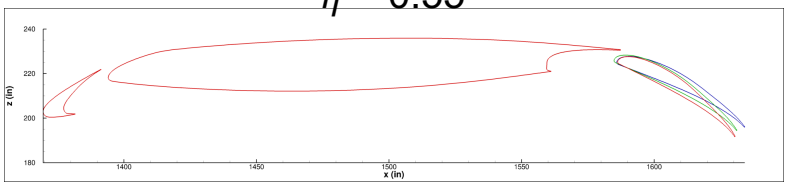


CRM-HL geometry

η = 0.24



η = 0.55

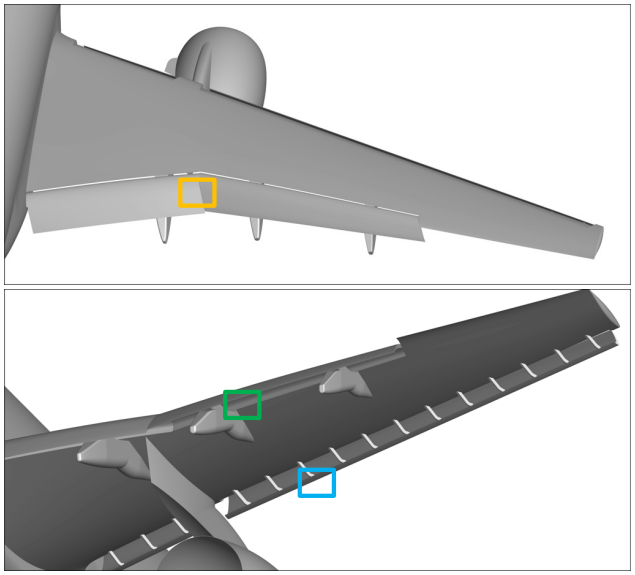


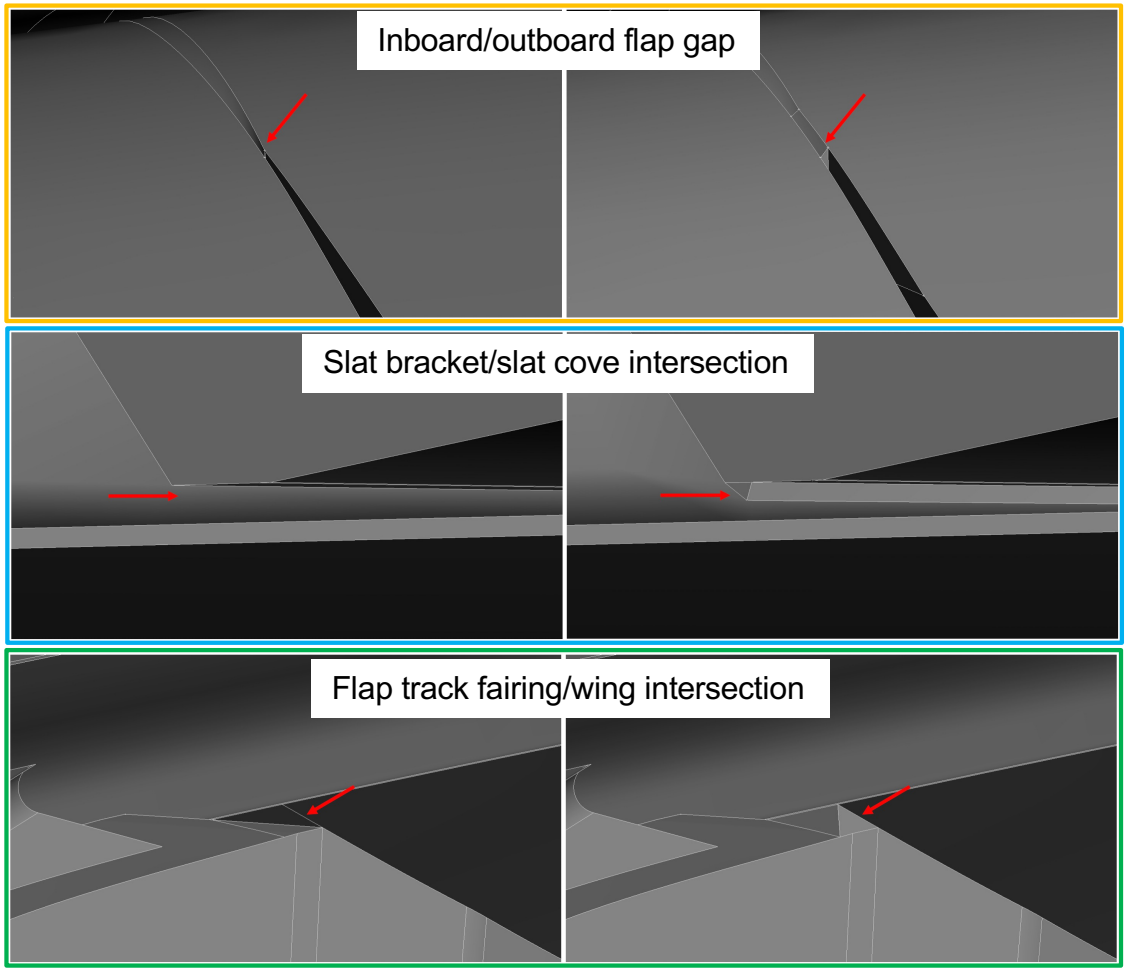
Sample CRM-HL airfoil profiles

[1]Lacy, D. S., and Clark, A. M., "Definition of Initial Landing and Takeoff Reference Configurations for the High Lift Common Research Model (CRM-HL)," AIAA AVIATION 2020 FORUM, 2020, p. 2771. https://doi.org/10.2514/6.2020-2771.

Methodology: Geometric Modifications

- Minor updates to the underlying geometry were necessary to allow *structured overset* mesh generation
- All modifications performed using the ANSA CAD software
- Sharp concave corners below a certain tolerance (~15º) removed to enable volume mesh extrusion
- Tight gaps widened to enable surface mesh topologies of acceptable quality

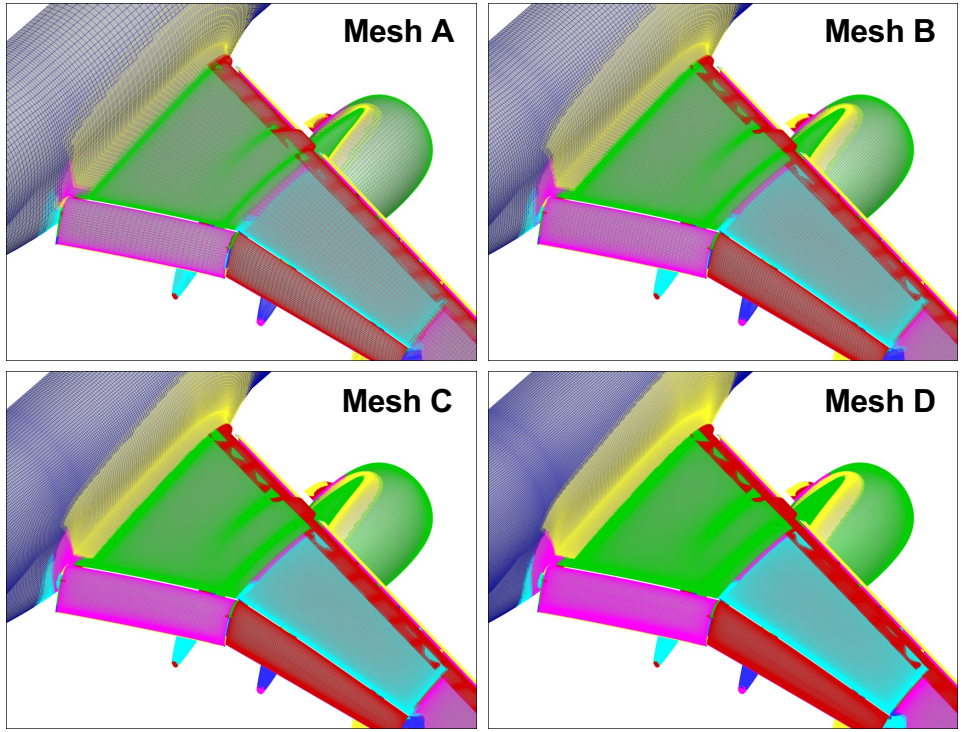




Methodology: Grid Generation

- Mesh generation completed using Pointwise and Chimera Grid Tools (CGT)
- Meshing strategy based on provided Geometry and Mesh Generation Workshop (GMGW-3) guidelines
- Point distributions and local refinement regions were adjusted based on initial CFD simulations
- Computational grids would serve as the official committee-provided structured overset mesh family

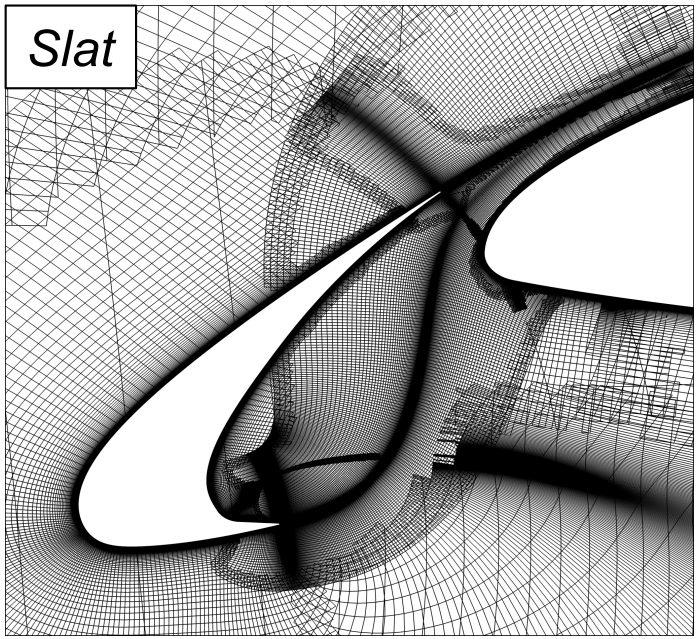
Mesh Level	Total Solve Points (M)	Target y^+	Max. Stretching Ratio
A	20.15	2.25	1.25
B	64.71	1.50	1.16
C	223.5	1.00	1.10
D	550.2	0.75	1.07

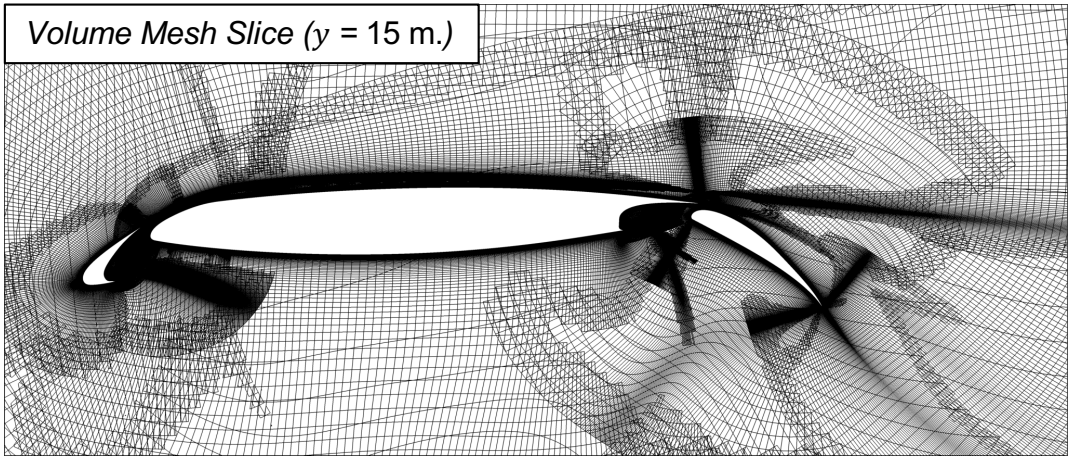


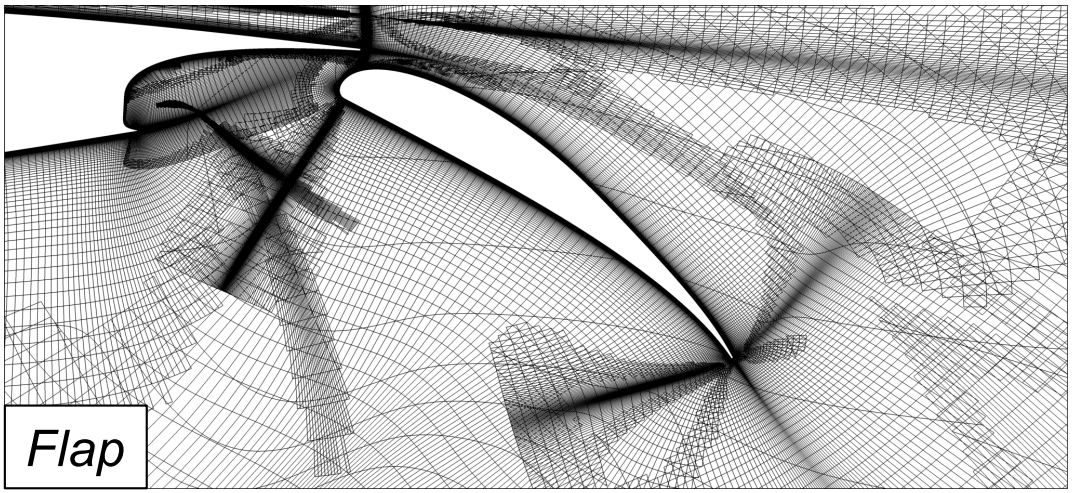
Free-air nominal configuration grid systems

Methodology: Grid Generation

- Wake refinement regions generated to better resolve higher gradients and separated flow regions
- Regions were refined downstream of all three wing element trailing edges (slats, wing, and flaps)
- Spatial extent and shaping of refinement regions determined based on preliminary RANS simulations

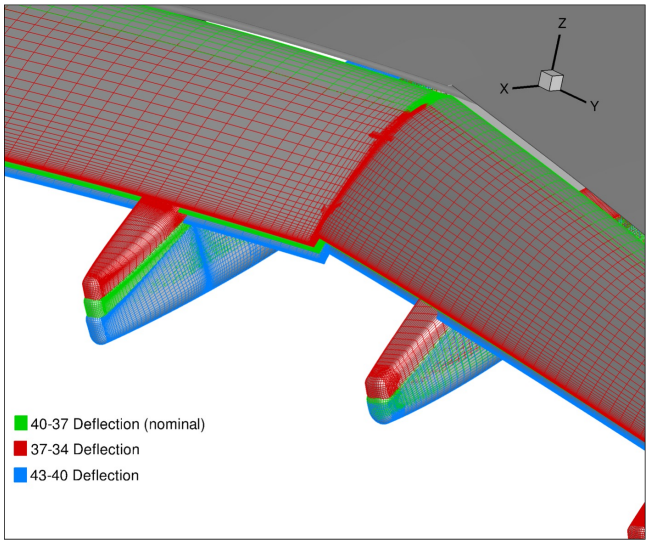




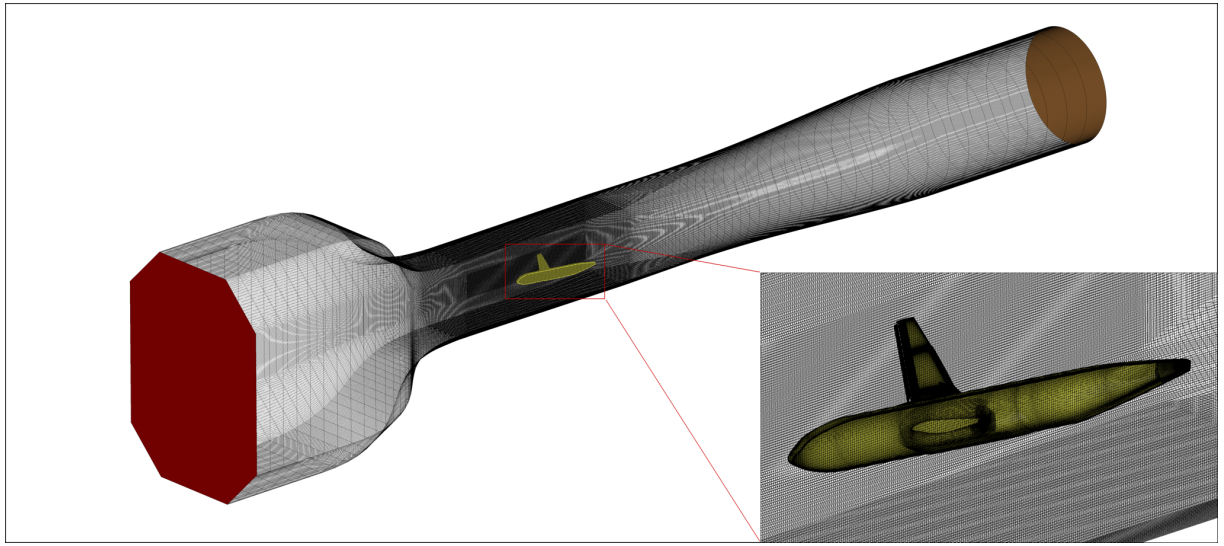


Methodology: Grid Generation

- Additional grid systems generated for workshop studies extending beyond nominal CRM-HL configuration
  - Flap deflection study grid systems (all refinement levels)
  - Wind tunnel modeling studies (mesh C equivalent refinement)
  - Reduced y^+ grid systems for coarsest refinement levels
- Unique grids required for each angle of attack for wind tunnel simulations



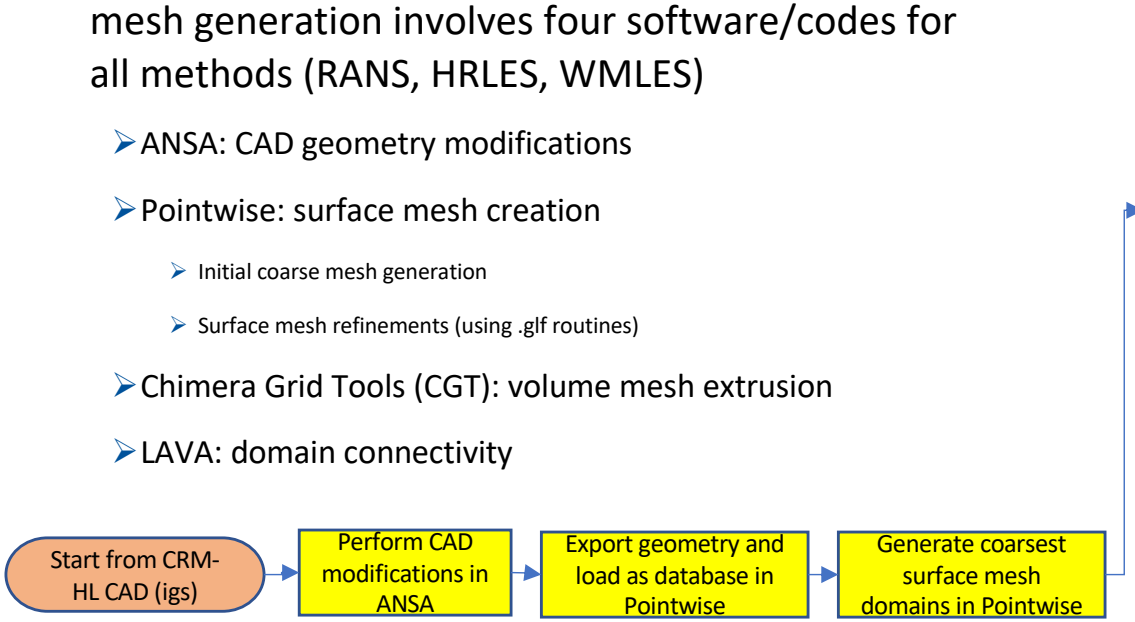
Flap deflection study grid systems

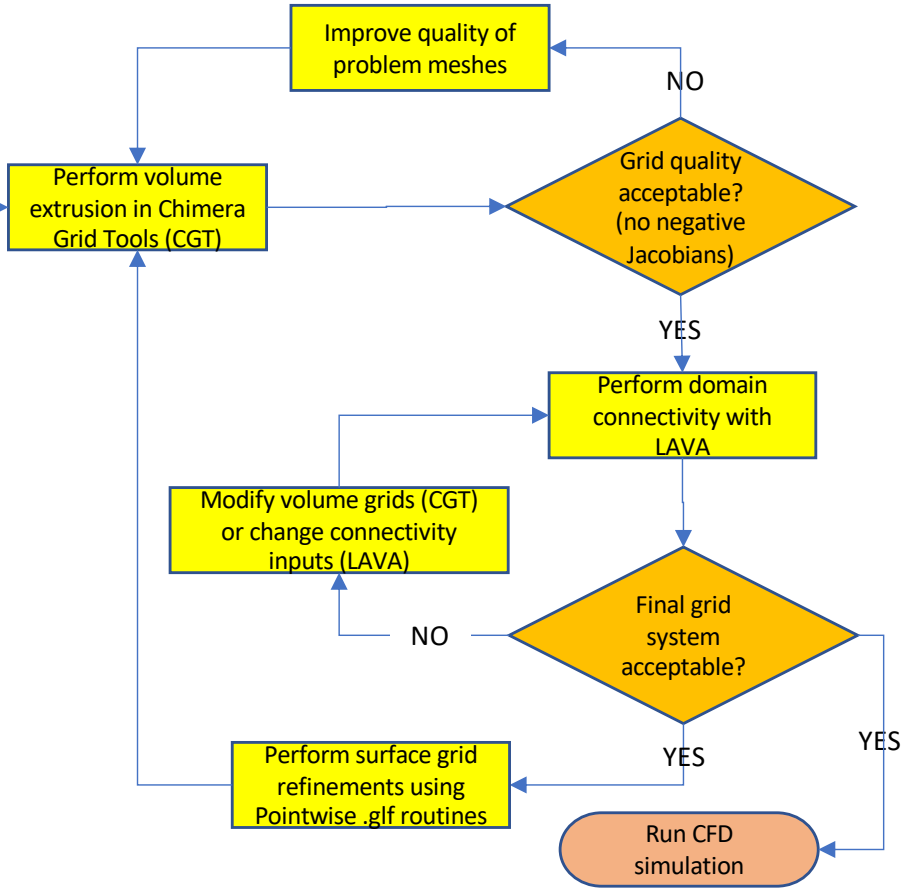


Wind tunnel modeling study grid system

Methodology: Grid Generation

- Complete process used for structured curvilinear mesh generation involves four software/codes for all methods (RANS, HRLES, WMLES)
  - ANSA: CAD geometry modifications
  - Pointwise: surface mesh creation
    - Initial coarse mesh generation
    - Surface mesh refinements (using .glf routines)
  - Chimera Grid Tools (CGT): volume mesh extrusion
  - LAVA: domain connectivity

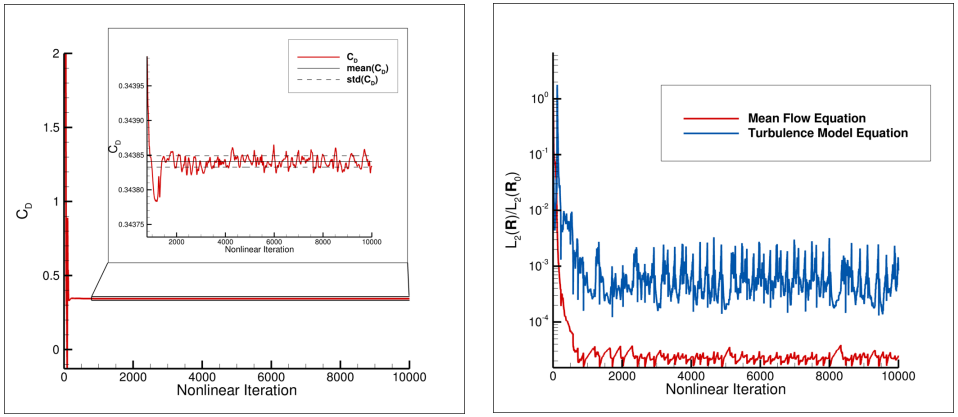




Methodology: Numerical Approach and Convergence

- All simulations solve the Reynolds-Averaged Navier-Stokes (RANS) using the Launch Ascent and Vehicle Aerodynamics (LAVA) solver
  - Modified Roe convective flux discretization
  - Numerous turbulence models explored (all cases assume fully-turbulent flow)
- Steady-state convergence criteria
  - Standard deviation of c_D in nonlinear iteration space is within 1e-5 and all loads are statistically stationary
  - All cases achieve 4-5 orders of mean flow equation residual reduction
  - Three averaging windows were used to guarantee that the reported drag values were accurate to within one drag count

Workshop Task	Turbulence model
Grid Convergence Study	SA, SA-RC-QCR2000
Flap Deflection Study	SA, SA-RC-QCR2000
c_{Lmax} Study	SA, SA-RC, SA-QCR2000, SA-RC-QCR2000, SA-LRe, k-ω BSL
Wind Tunnel Simulations	SA

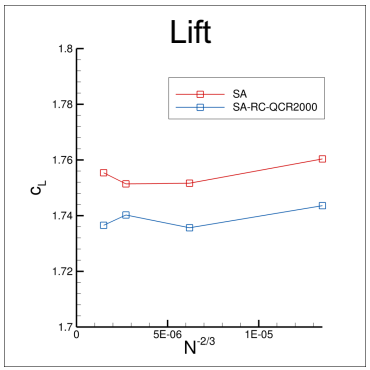


Sample steady-state convergence histories. L_2 norm of the residual of the NS equations in strong conservation law form includes residuals of mass, momentum, and energy.

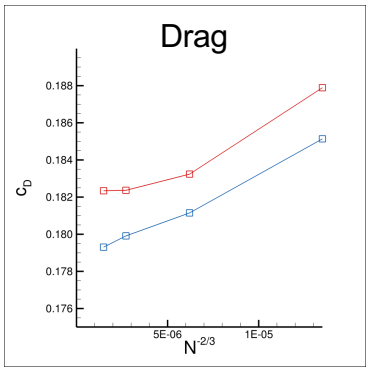
Grid Convergence Study: Aerodynamic Quantities

- Sensitivity of solution to mesh resolution assessed using two variants of the SA turbulence model at α = 7.05º
- Differences in quantities between finest resolutions (C and D) within 0.9%
- Baseline SA demonstrates best agreement with experiment

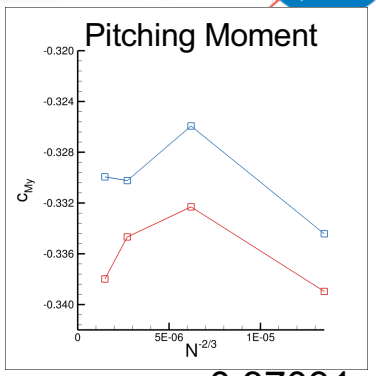
Mesh Level	c_L (SA)	% Diff. from experiment	c_L (SA-RC-QCR2000)	% Diff. from experiment
A	1.7604	1.03	1.7436	1.97
B	1.7517	1.52	1.7357	2.42
C	1.7514	1.53	1.7402	2.16
D	1.7554	1.31	1.7365	2.37



$c_{L,exp}$ = 1.7786

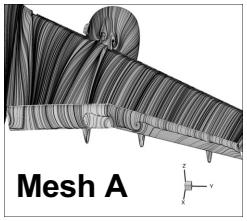


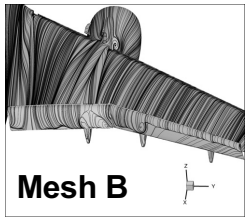
$c_{D,exp}$ = 0.18671

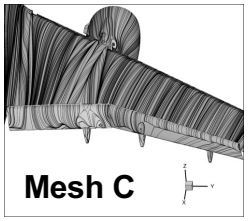


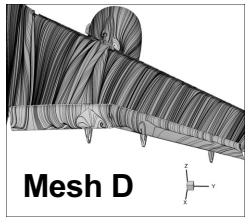
$c_{My,exp}$ = -0.37031

Baseline SA

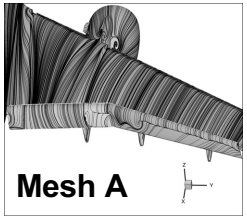


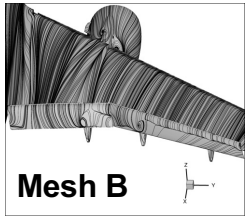


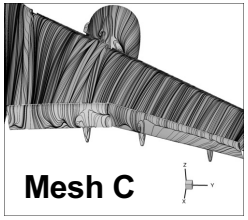


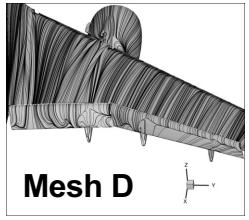


SA-RC-QCR2000



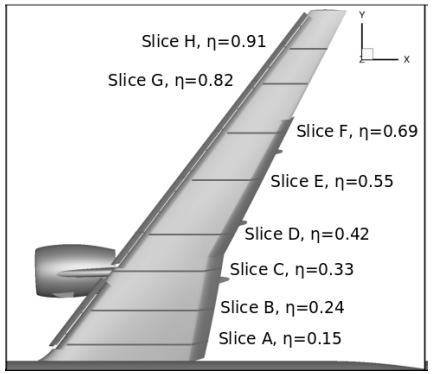


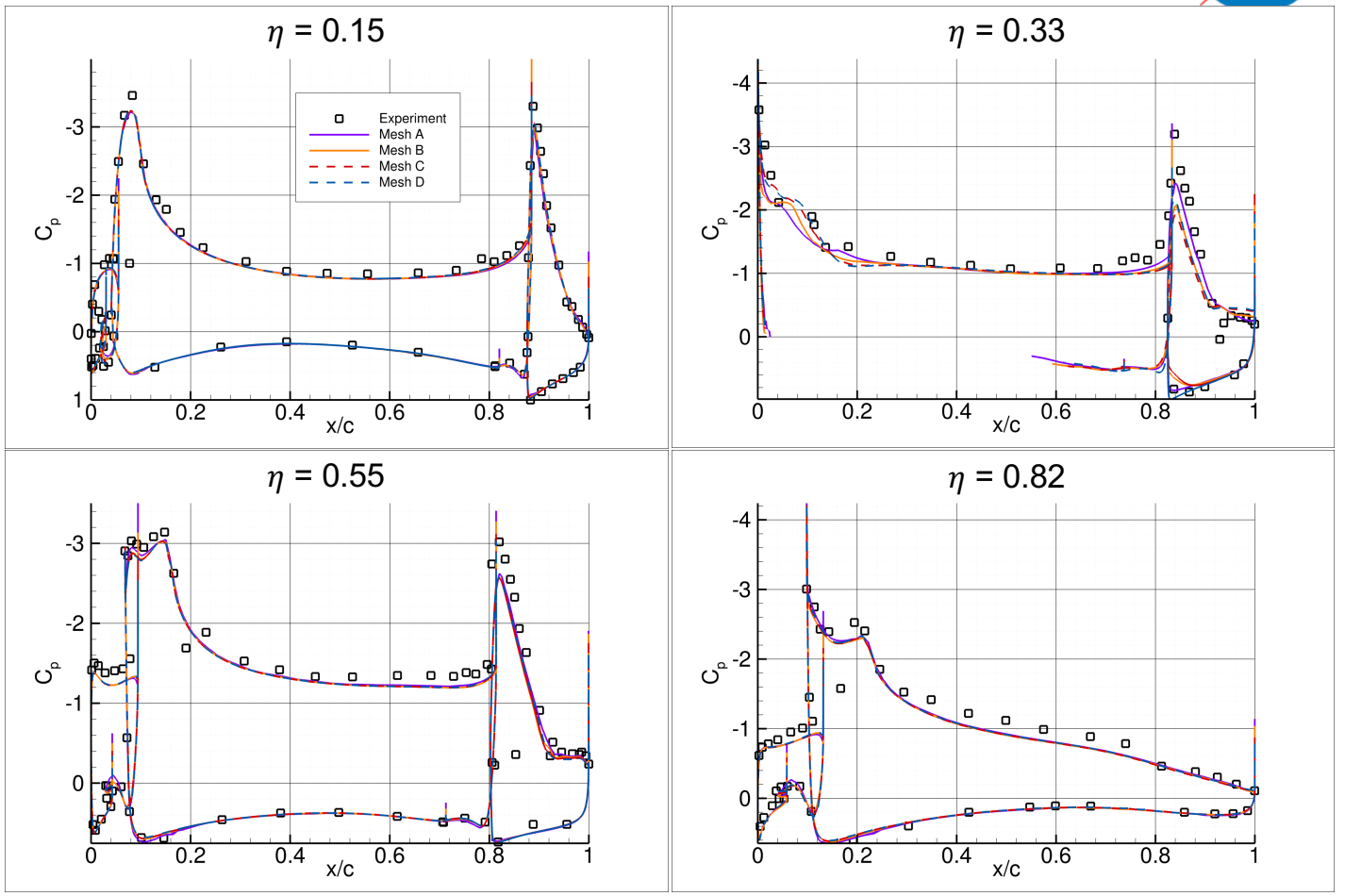




Grid Convergence Study: Pressure Distributions

- Sensitivity of pressure to mesh resolution assessed using the baseline SA turbulence model at α = 7.05º
- All resolutions generally underpredict suction side pressure distributions
- Variation most pronounced in nacelle/pylon wake spanwise location

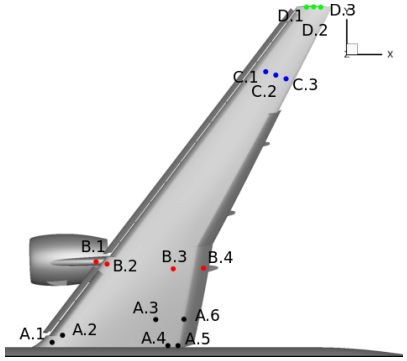


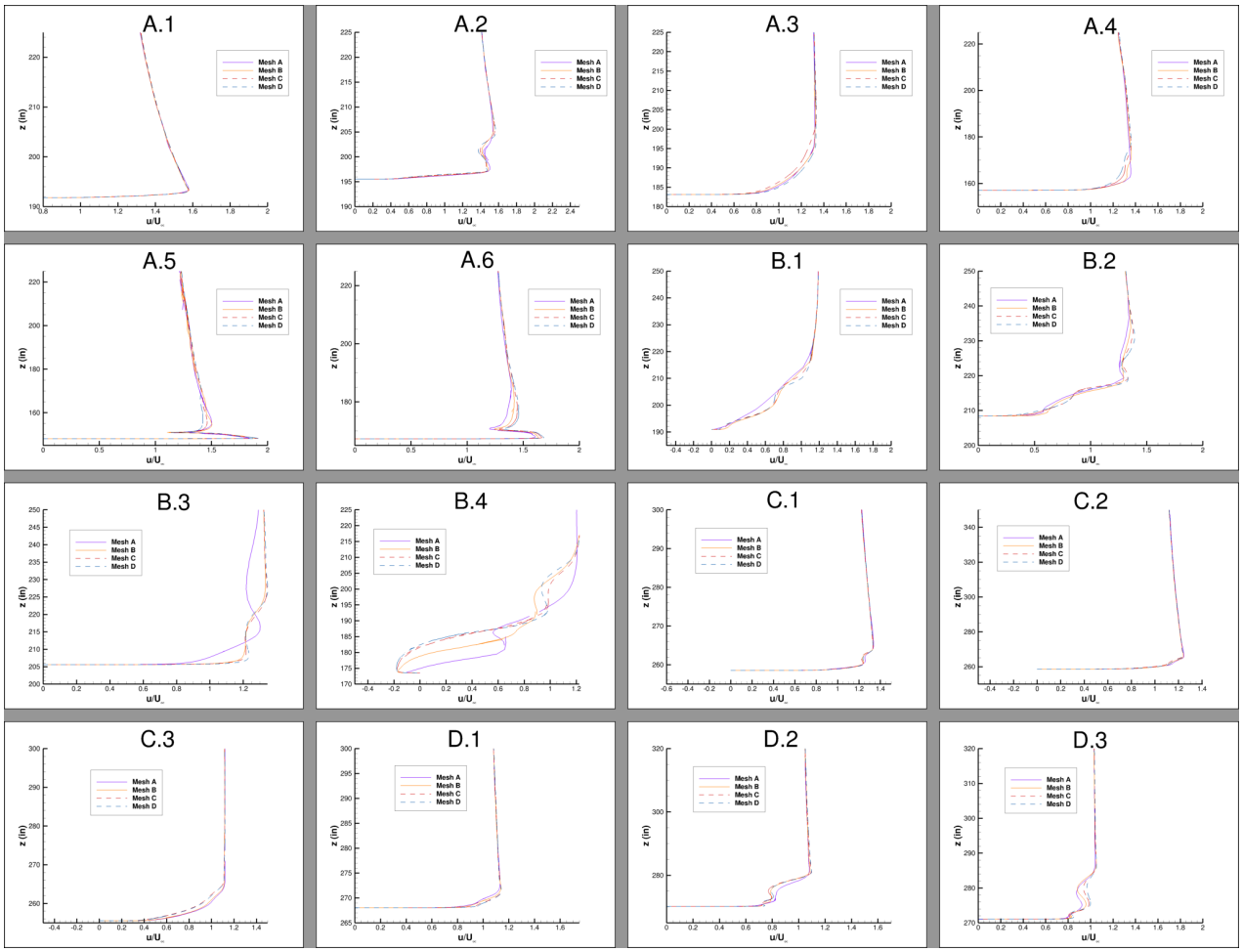


Pressure distributions at α = 7.05º using the baseline SA turbulence model

Grid Convergence Study: Velocity Profiles

- Sensitivity of boundary layer velocity profiles to mesh resolution assessed using the baseline SA turbulence model at α = 7.05º
- Variation most pronounced in nacelle/pylon wake spanwise location

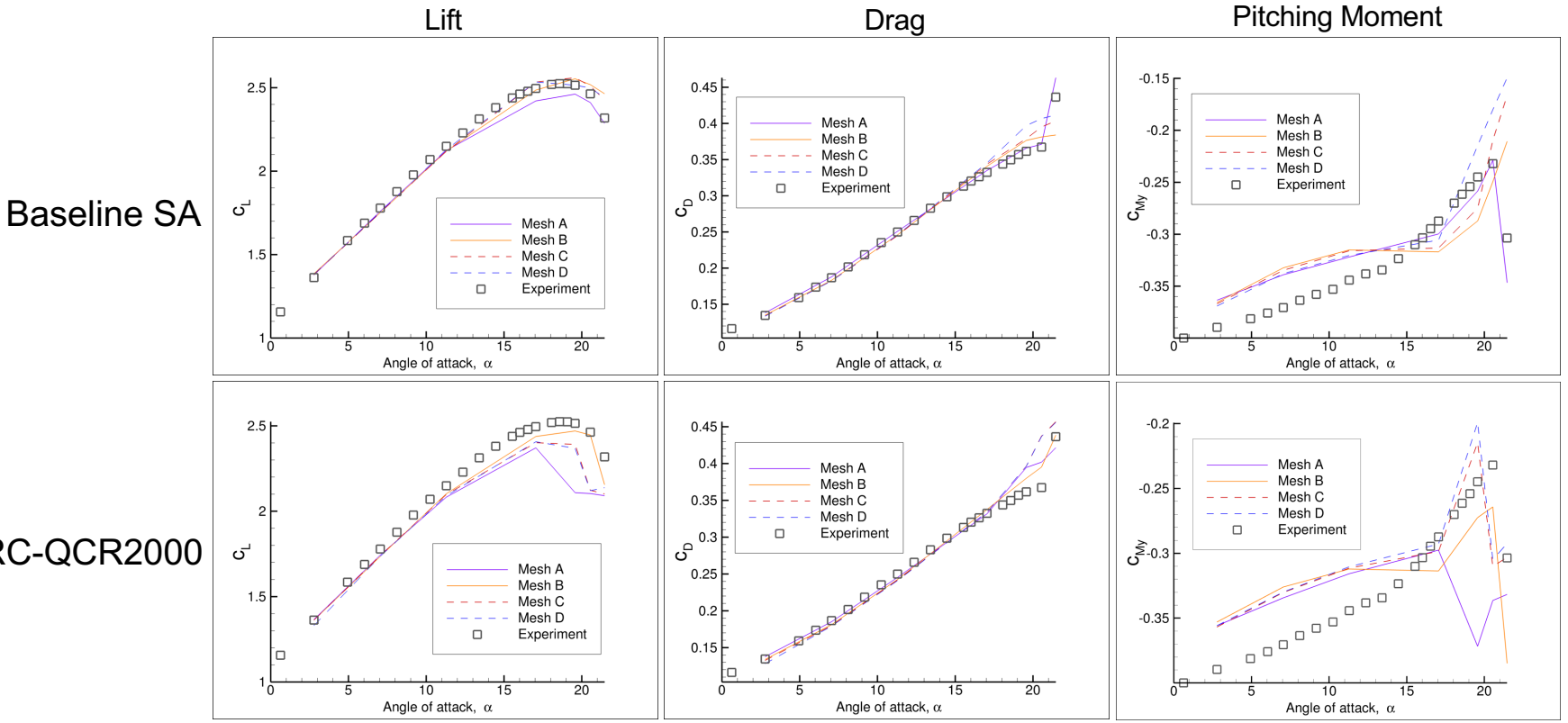




Velocity profiles at α = 7.05º using the baseline SA turbulence model

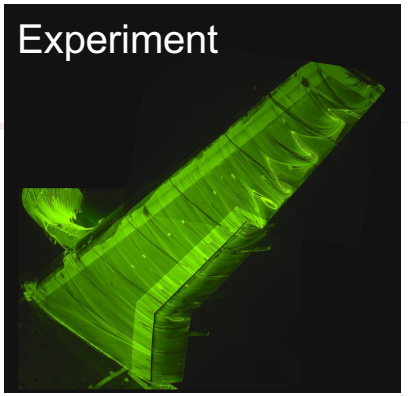
Grid Convergence Study: α-Sweep

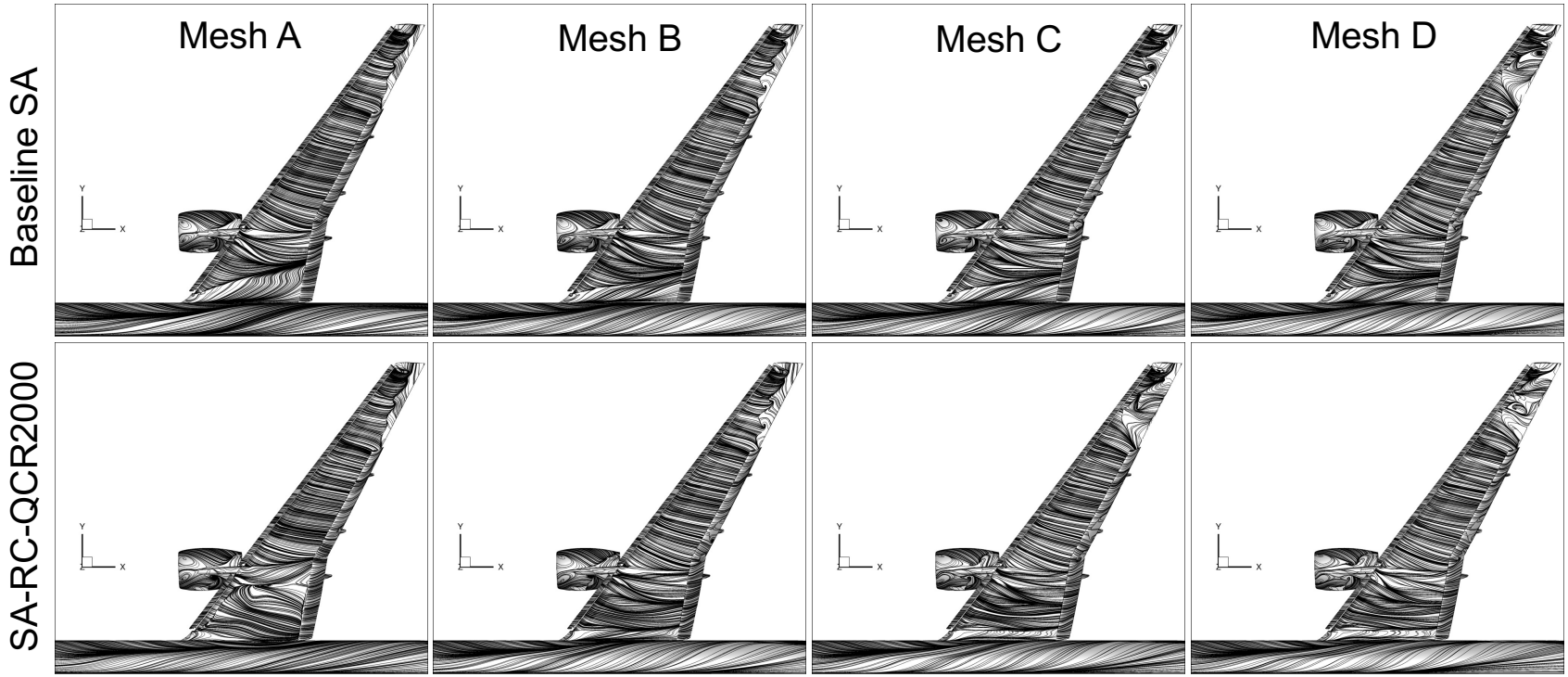
- Mesh sensitivity study extended beyond the low-α regime to assess solution sensitivity at near-stall angles of attack
- Integrated quantity spread increases substantially just before the experimental c_{Lmax}



Grid Convergence Study

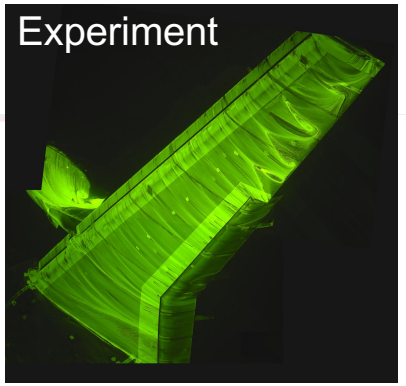
- Mesh sensitivity study extended beyond the low-α regime to assess solution sensitivity at near-stall angles of attack
- Surface streamlines for each mesh resolution at α = 19.57º visualized

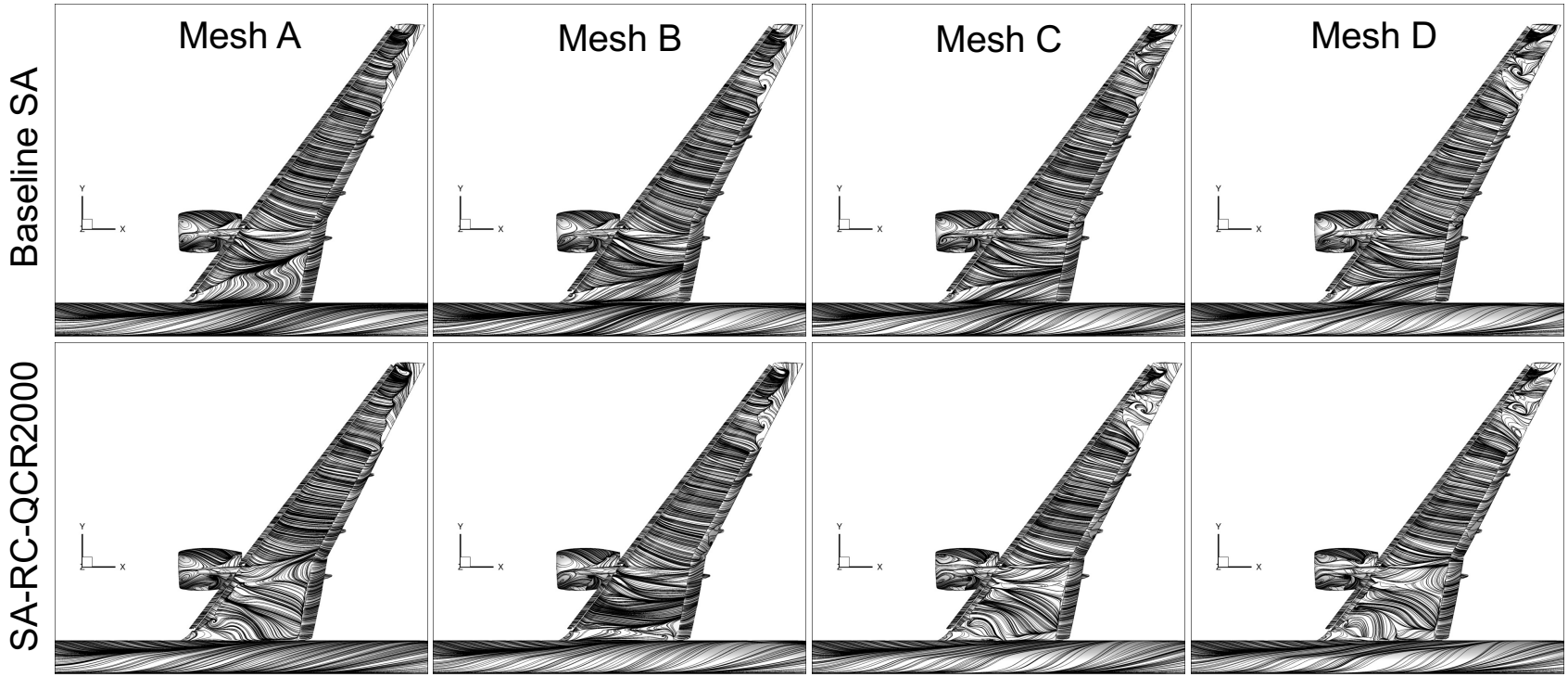




Grid Convergence Study

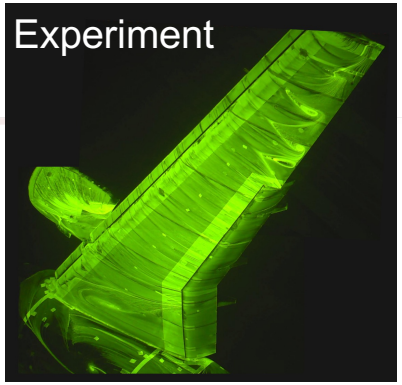
- Mesh sensitivity study extended beyond the low-α regime to assess solution sensitivity at near-stall angles of attack
- Surface streamlines for each mesh resolution at α = 20.55º visualized

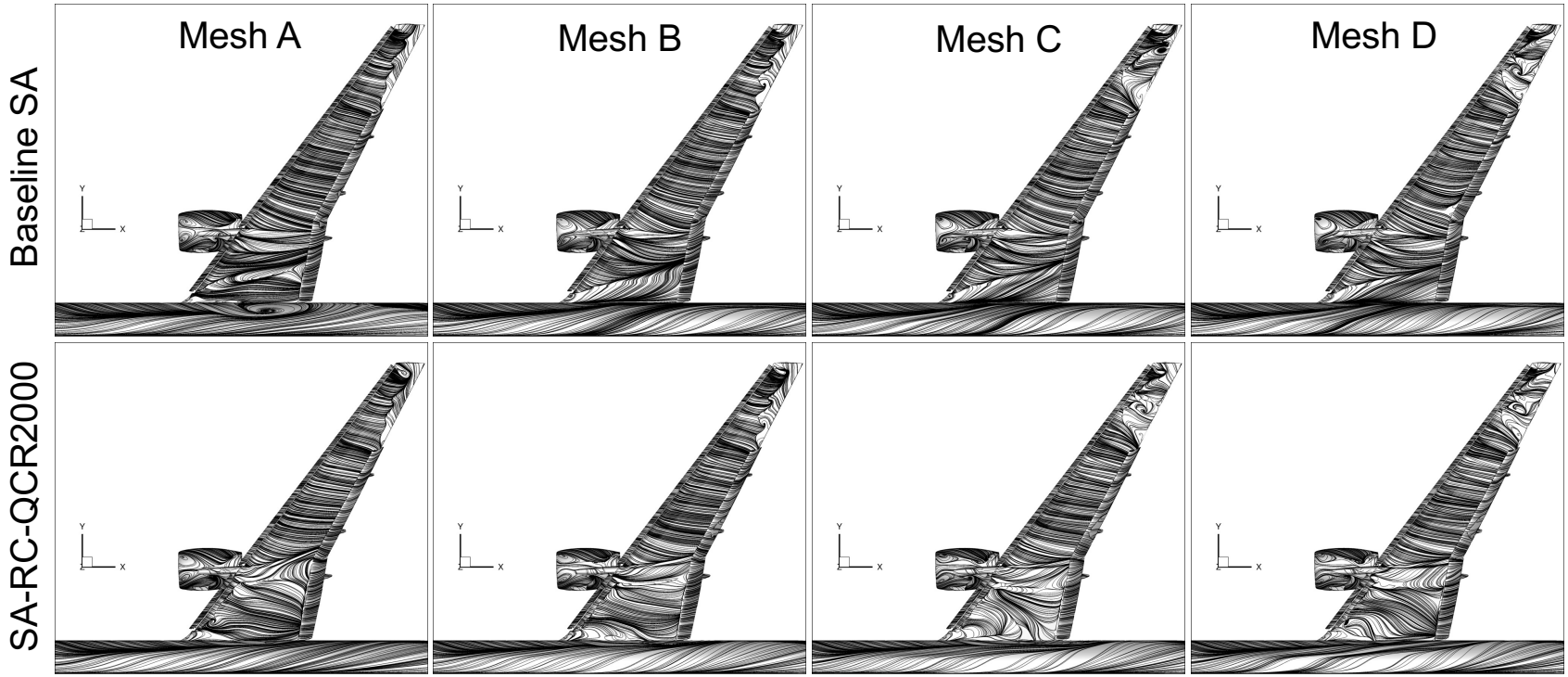




Grid Convergence Study

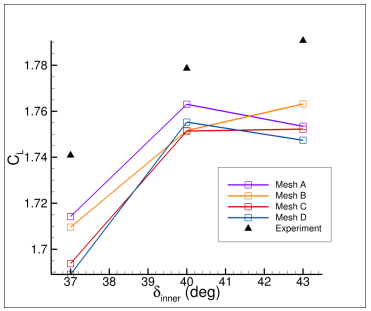
- Mesh sensitivity study extended beyond the low-α regime to assess solution sensitivity at near-stall angles of attack
- Surface streamlines for each mesh resolution at α = 21.47º visualized



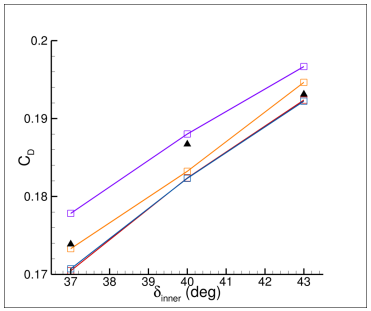


Flap Deflection Study

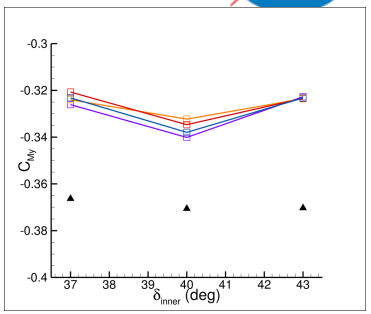
- Baseline SA and SA-RC-QCR2000 (not shown) models used to predict flap deflection increments at α = 7.05º
- Mesh levels B and C results using SA do not predict a negative Δc_L between the highest deflections
- Minor differences between resolutions C and D



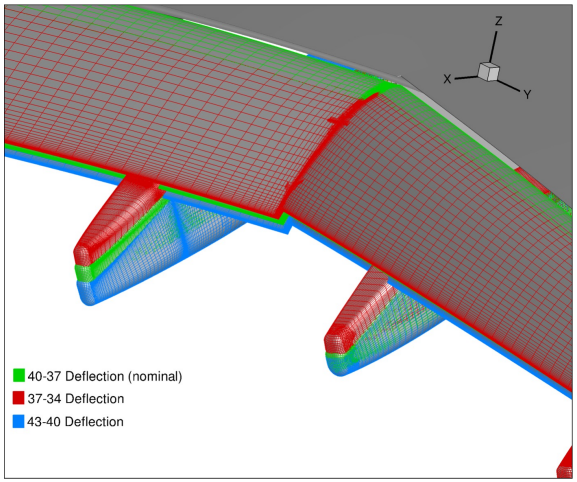
Lift

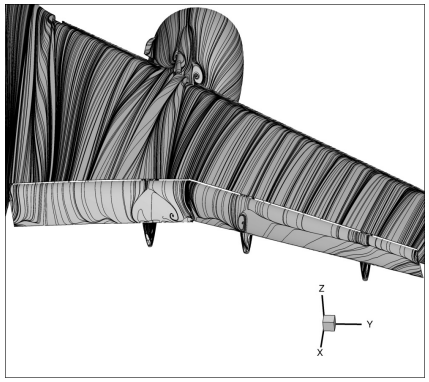


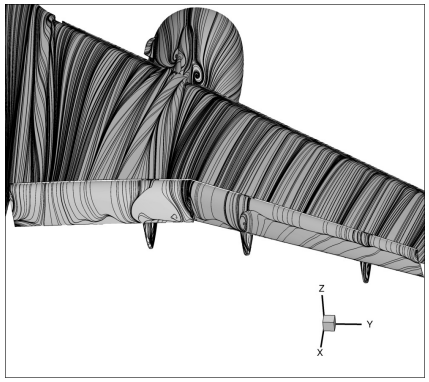
Drag

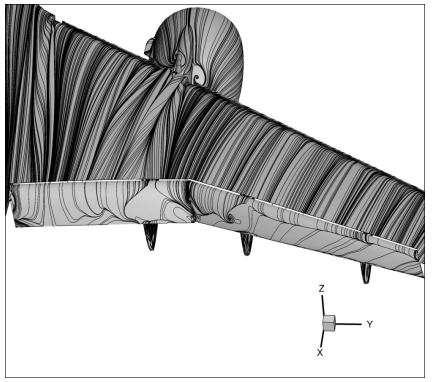


Pitching Moment




$\delta_f = 37°/34°$


$\delta_f = 40°/37°$

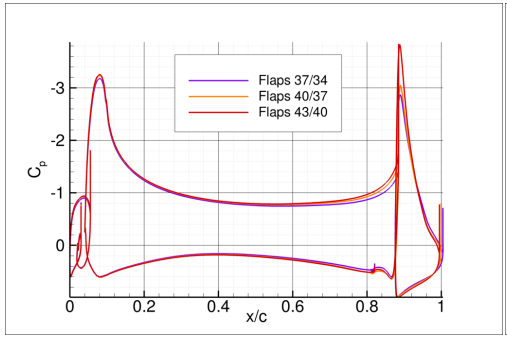

$\delta_f = 43°/40°$

Streamlines shown for each deflection at mesh level C.

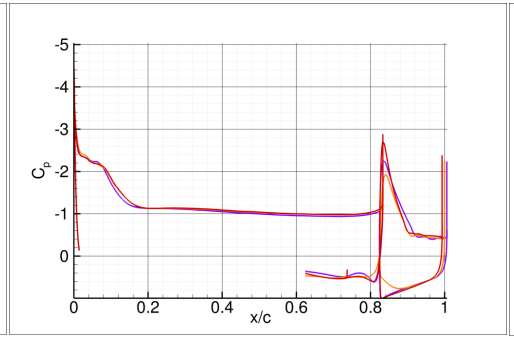
Flap Deflection Study

- Pressure distributions visualized for each deflection on mesh level C
- Baseline SA and SA-RC-QCR2000 both exhibit highest sensitivity on flap element, particularly at outboard locations
- Incompressible nature of flow causes upstream effects on other wing elements

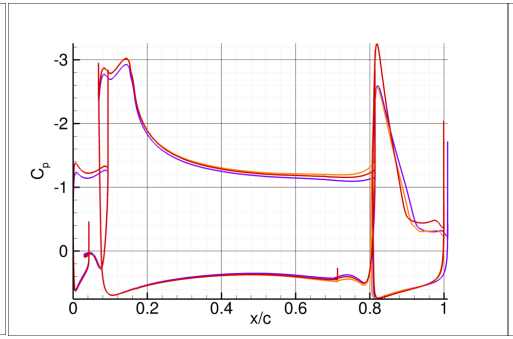
Baseline SA



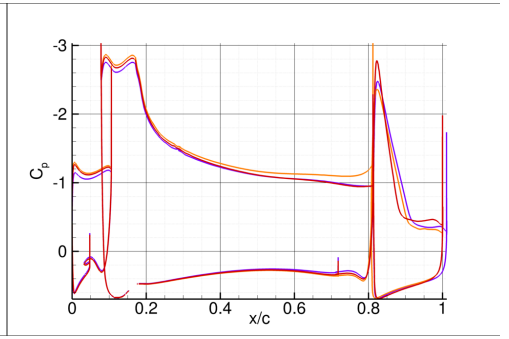
η = 0.15



η = 0.33

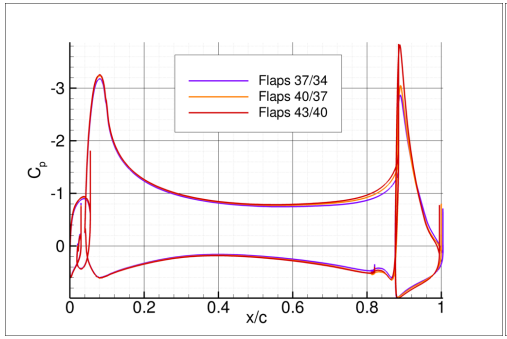


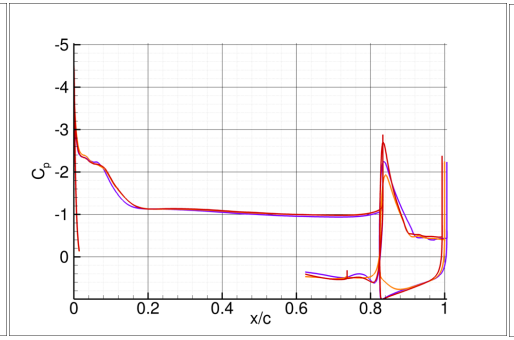
η = 0.55

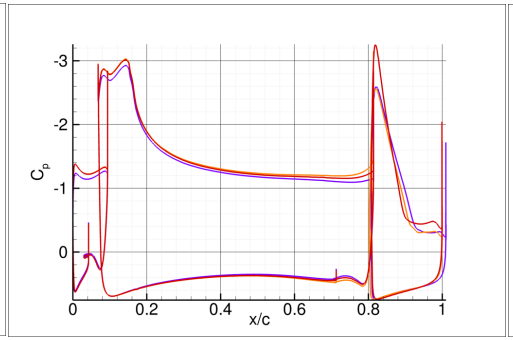


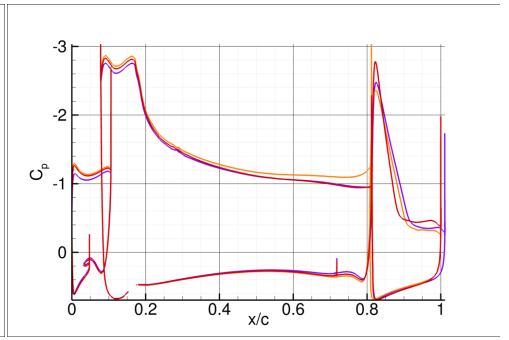
η = 0.69

SA-RC-QCR2000



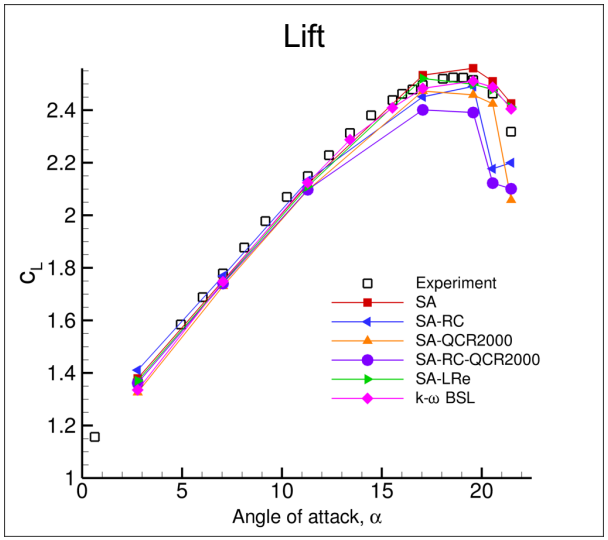


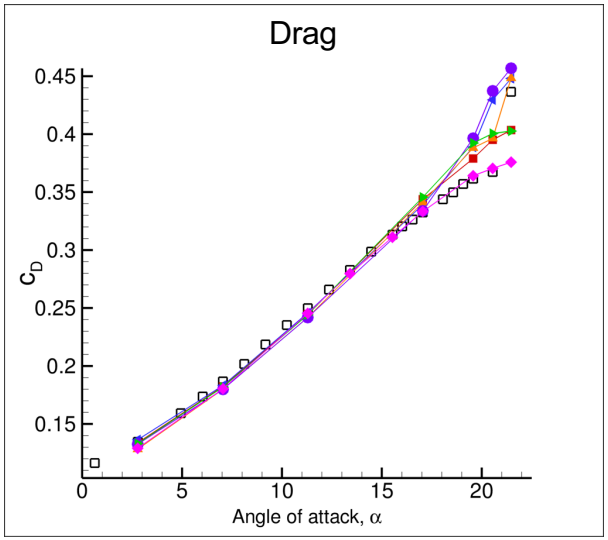


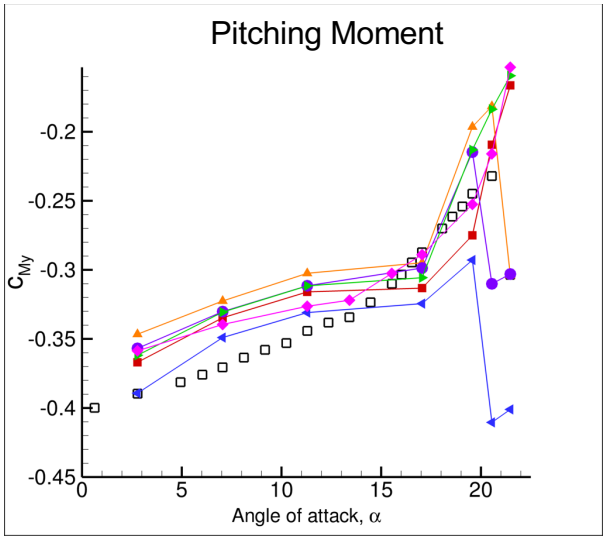


c_{Lmax} Study: Turbulence Model Sensitivity

- Six turbulence models were assessed using mesh level C (5 SA variants and k-ω BSL)
- Simulations demonstrate unique characteristics at high-α conditions, including the presence of a high-α pitch break captured in the experiment
- Corrections to SA model generally lead to underprediction of high-α lift at varying degrees
- Error in predicted c_{Lmax} relative to experiment ranging from 0.2% to 4.9% (0.2% to 1.8% excluding QCR2000 predictions)

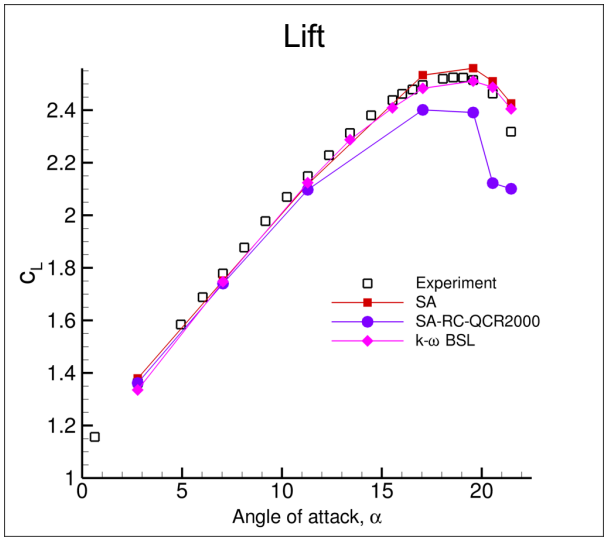


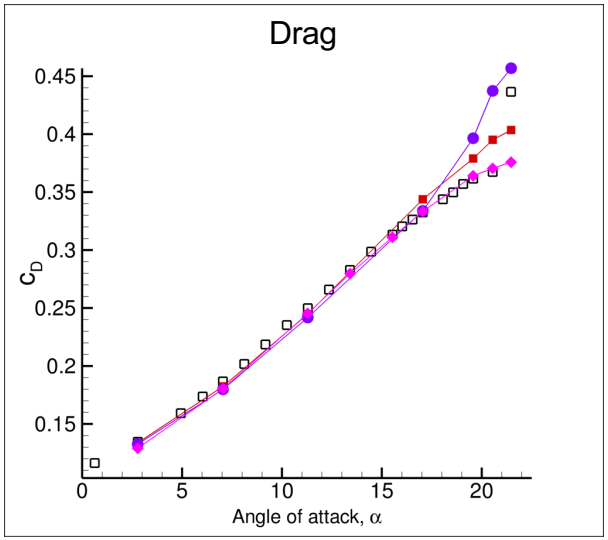


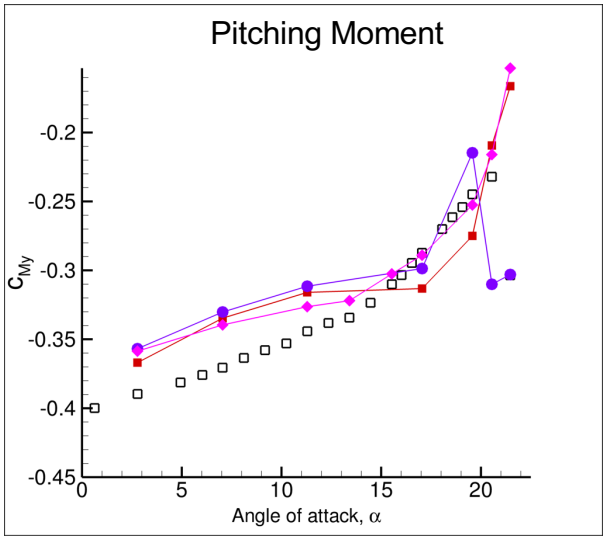


c_{Lmax} Study: Turbulence Model Sensitivity

- Six turbulence models were assessed using mesh level C (5 SA variants and k-ω BSL)
- Simulations demonstrate unique characteristics at high-α conditions, including the presence of a high-α pitch break captured in the experiment
- Corrections to SA model generally lead to underprediction of high-α lift at varying degrees
- Error in predicted c_{Lmax} relative to experiment ranging from 0.2% to 4.9% (0.2% to 1.8% excluding QCR2000 predictions)



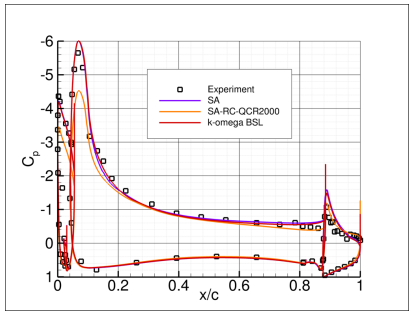




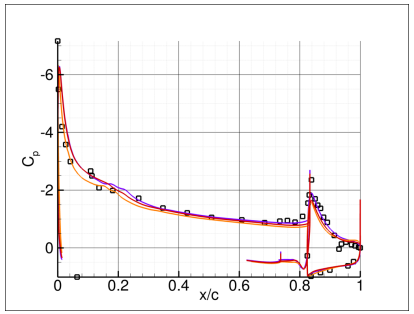
c_{Lmax} Study: Turbulence Model Sensitivity

- Pressure distributions analyzed for perceived “best” and “worst” performing models with respect to c_{Lmax} prediction
- SA-RC-QCR2000 struggles to predict outboard pressure at high-α, but captures collapse of inboard suction peak at α = 21.47º
- Baseline SA and k-ω BSL both struggle to predict suction side pressure at inboard-most location

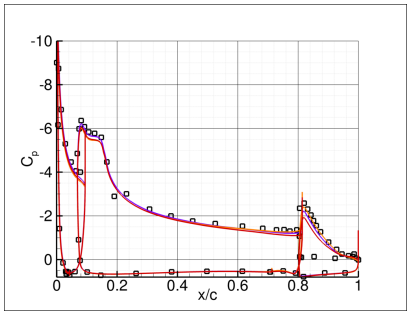
α = 19.57º



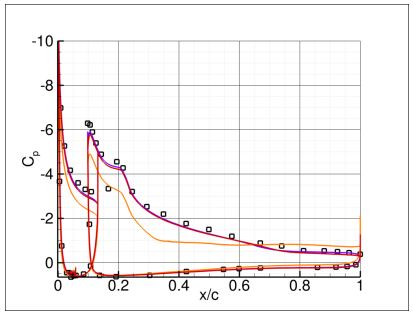
η = 0.15



η = 0.33

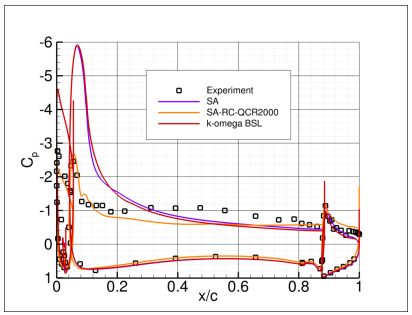


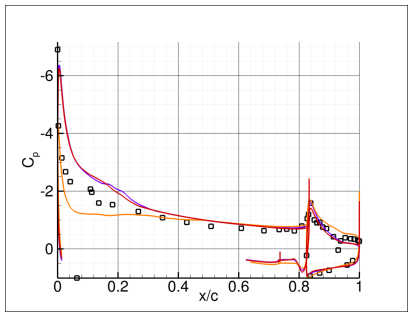
η = 0.55

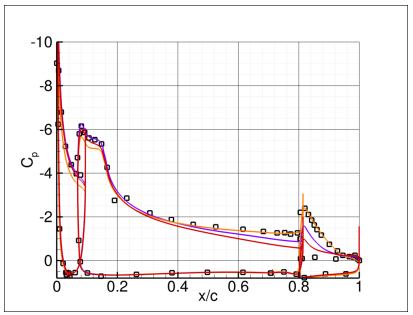


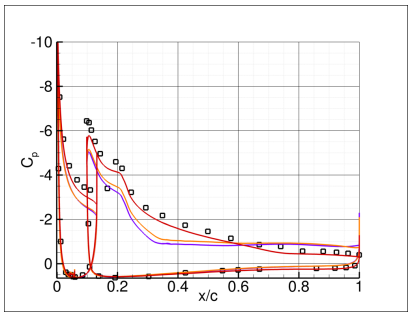
η = 0.82

α = 21.47º



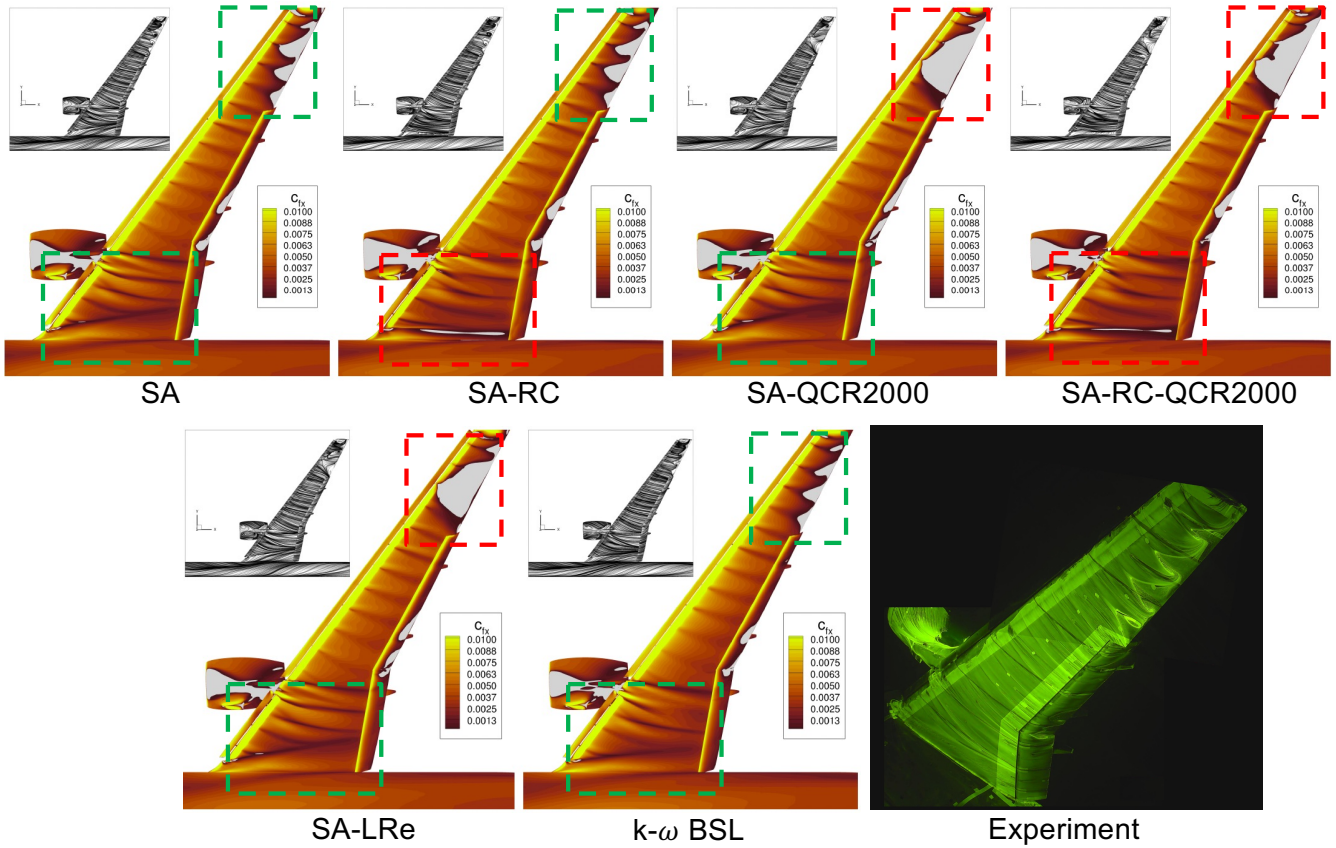






c_{Lmax} Study: Turbulence Model Sensitivity

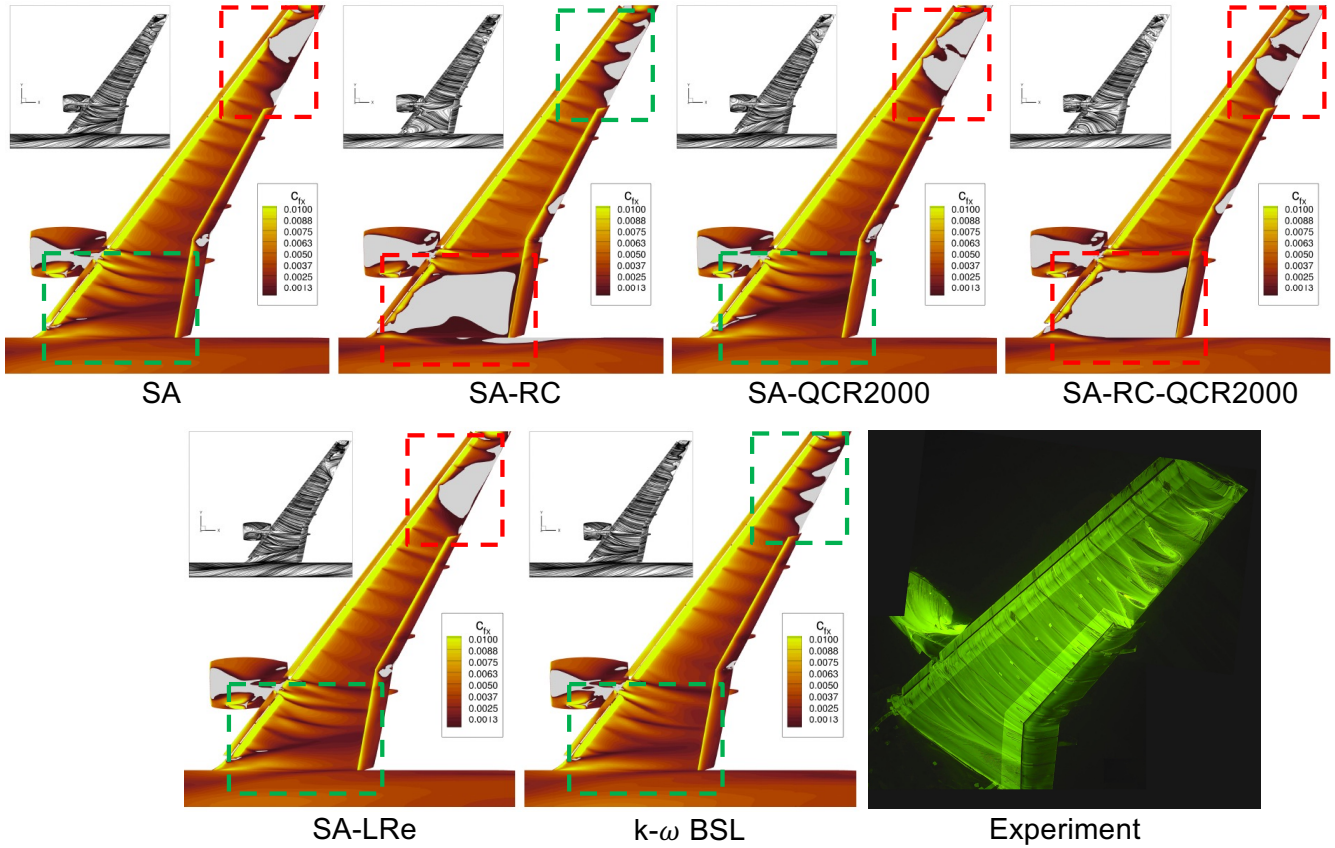
- Six turbulence models were assessed using mesh level C (5 SA variants and k-ω BSL)
- Solutions demonstrate unique characteristics at the α = 19.57º condition (right image)
- Corrections to SA model generally lead to mispredictions in the inboard (RC correction) and outboard topologies (QCR2000 and LRe corrections)



x-component of skin friction (C_{fx}) with surface streamlines shown in inset image

c_{Lmax} Study: Turbulence Model Sensitivity

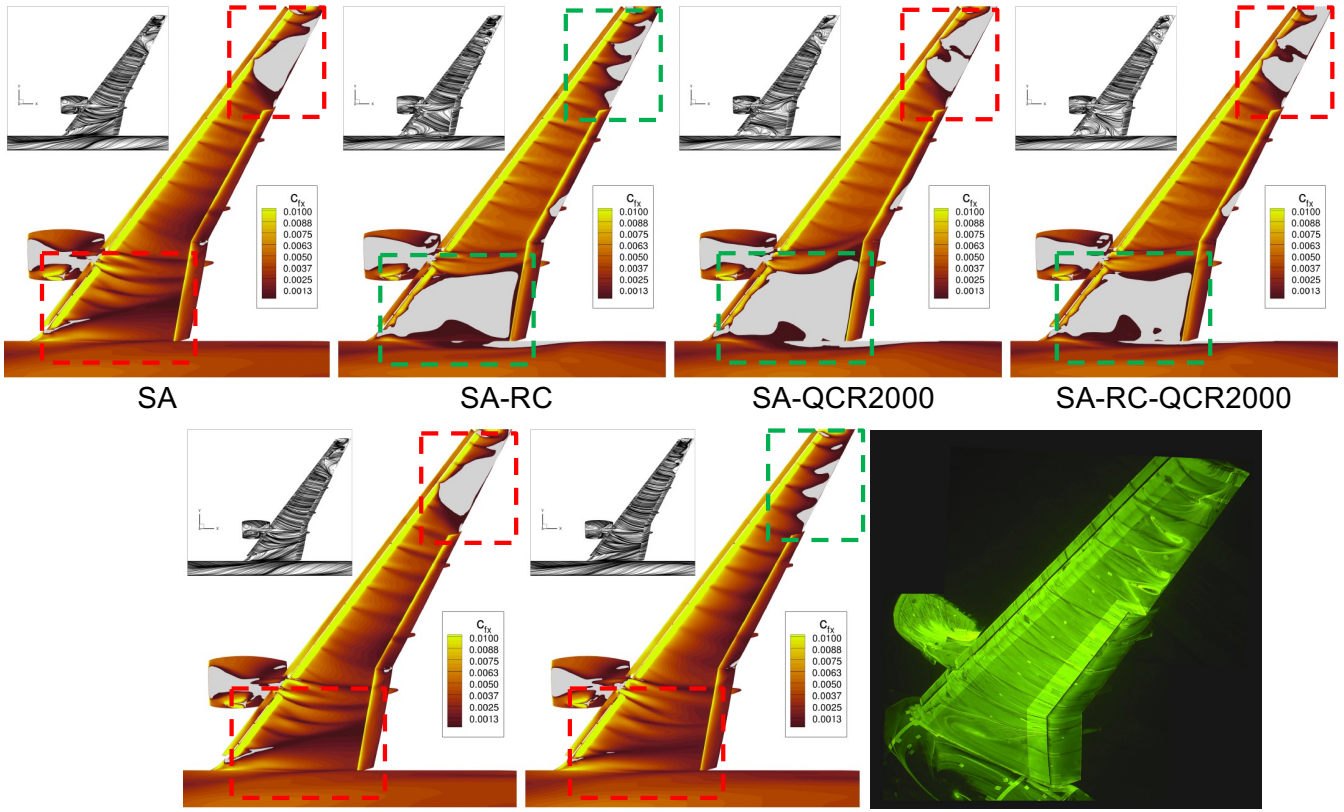
- Six turbulence models were assessed using mesh level C (5 SA variants and k-ω BSL)
- Solutions demonstrate unique characteristics at the α = 20.55º condition (right image)
- RC correction produces early onset of inboard separation
- Nearly all SA variants produce spurious outboard separation



x-component of skin friction (C_{fx}) with surface streamlines shown in inset image

c_{Lmax} Study: Turbulence Model Sensitivity

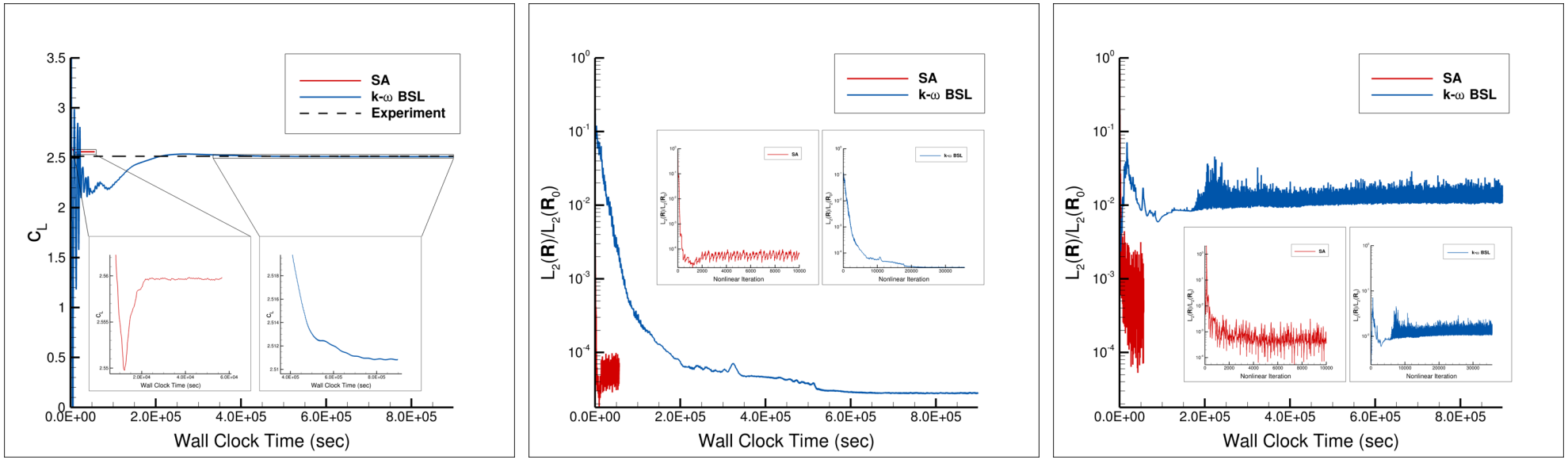
- Six turbulence models were assessed using mesh level C (5 SA variants and k-ω BSL)
- Solutions demonstrate unique characteristics at the α = 21.47º condition (right image)
- Most corrections to SA model correctly predict qualitative inboard separation
- SA-RC and k-ω BSL only models to predict correct outboard topology



x-component of skin friction (C_{fx}) with surface streamlines shown in inset image

c_{Lmax} Study: Turbulence Model Sensitivity

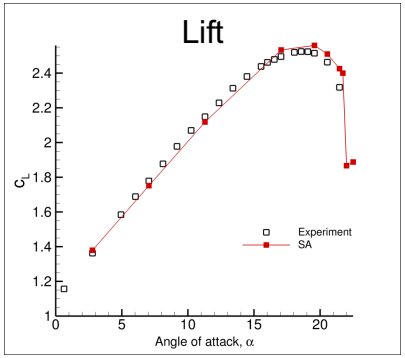
- Accuracy of k-ω BSL arguably highest relative to other closures, with baseline SA performing well relative to other SA variants
- Computational performance of the baseline SA and k-ω BSL turbulence models compared for the α = 19.57º condition
- Required wall clock time of k-ω BSL is about 10-15X higher than baseline SA (using current convergence criteria) in our framework

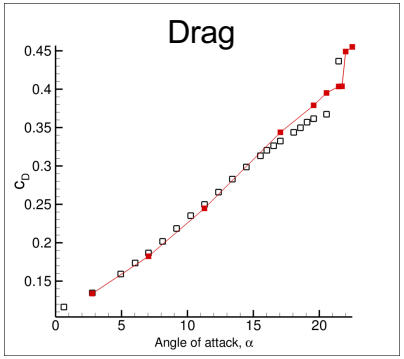


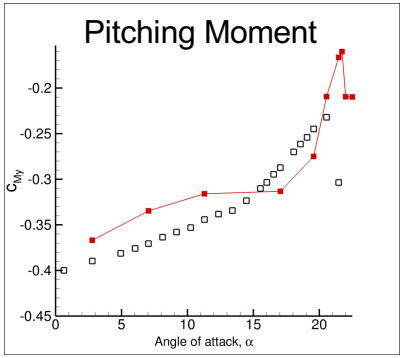
Sample convergence histories for baseline SA and k-ω BSL simulations

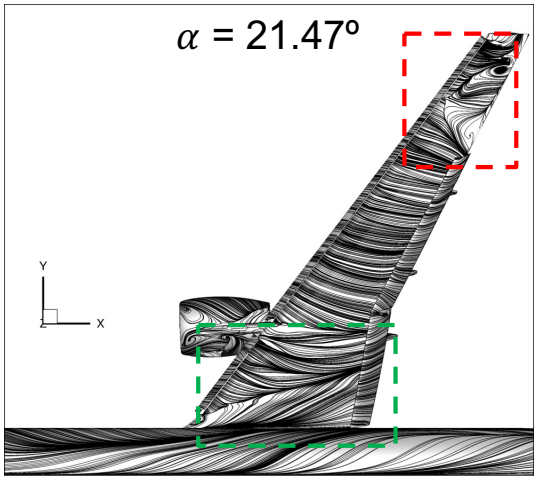
c_{Lmax} Study: Extension of Baseline SA Sweep

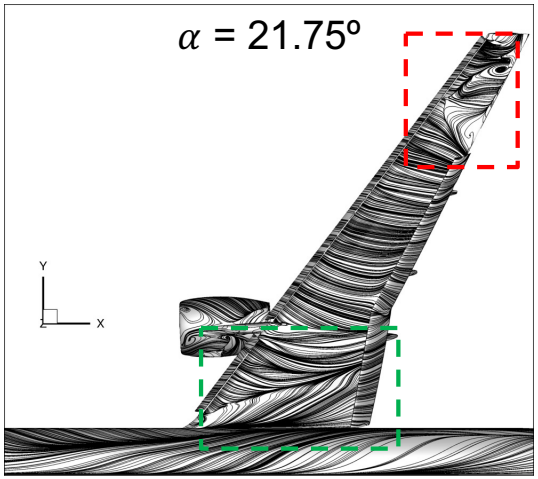
- Additional angles of attack past the highest requested workshop angle were simulated to attempt to recover the pitch break at high- α
- Corner flow separation-induced pitch break obtained at α = 22.00º
- Other spurious separation regions arise and persist

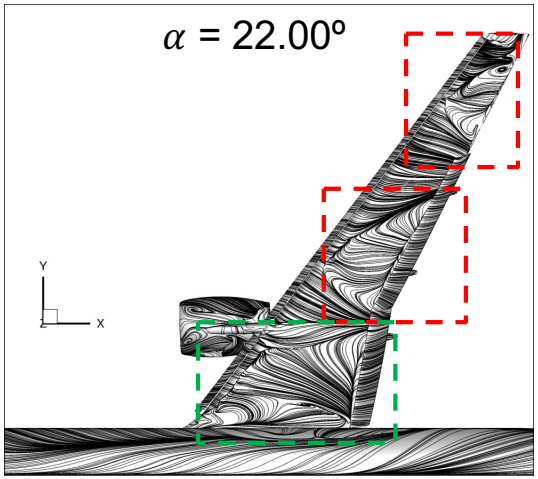








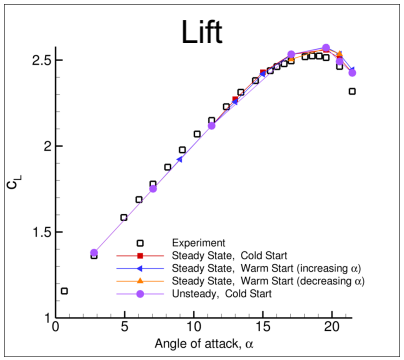


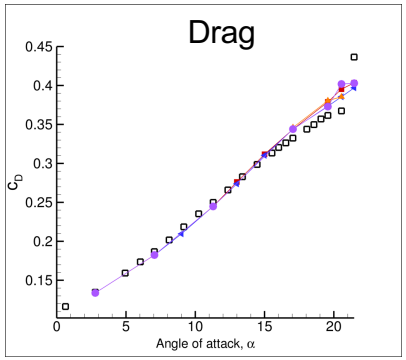


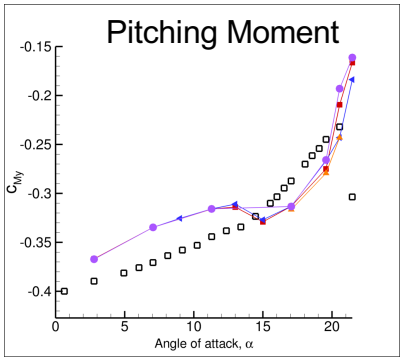
Surface streamlines at selected angles of attack

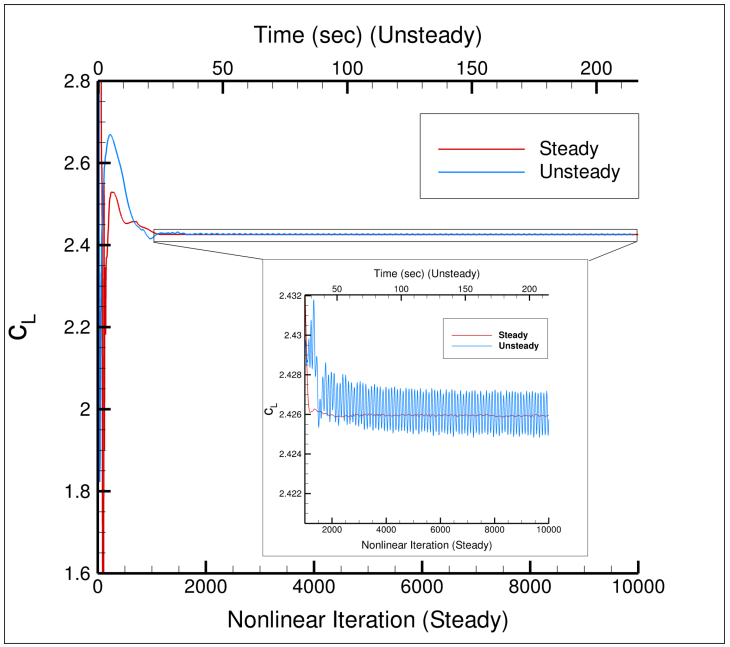
c_{Lmax} Study: Alternative Solution Methods

- Additional simulation methods utilized in attempt to improve baseline SA predictions at high-α
  - Unsteady RANS, cold start
  - Steady RANS, warm start (increasing α)
  - Steady RANS, warm start (decreasing α)
- Overall spread not as pronounced near c_{Lmax} as observed in other sensitivity studies
- High- α pitch break still not produced with any alternative simulation methodology





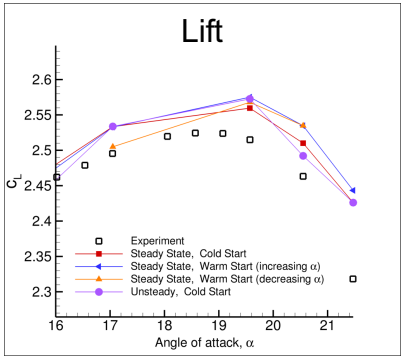


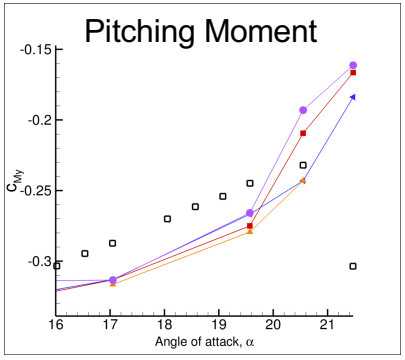


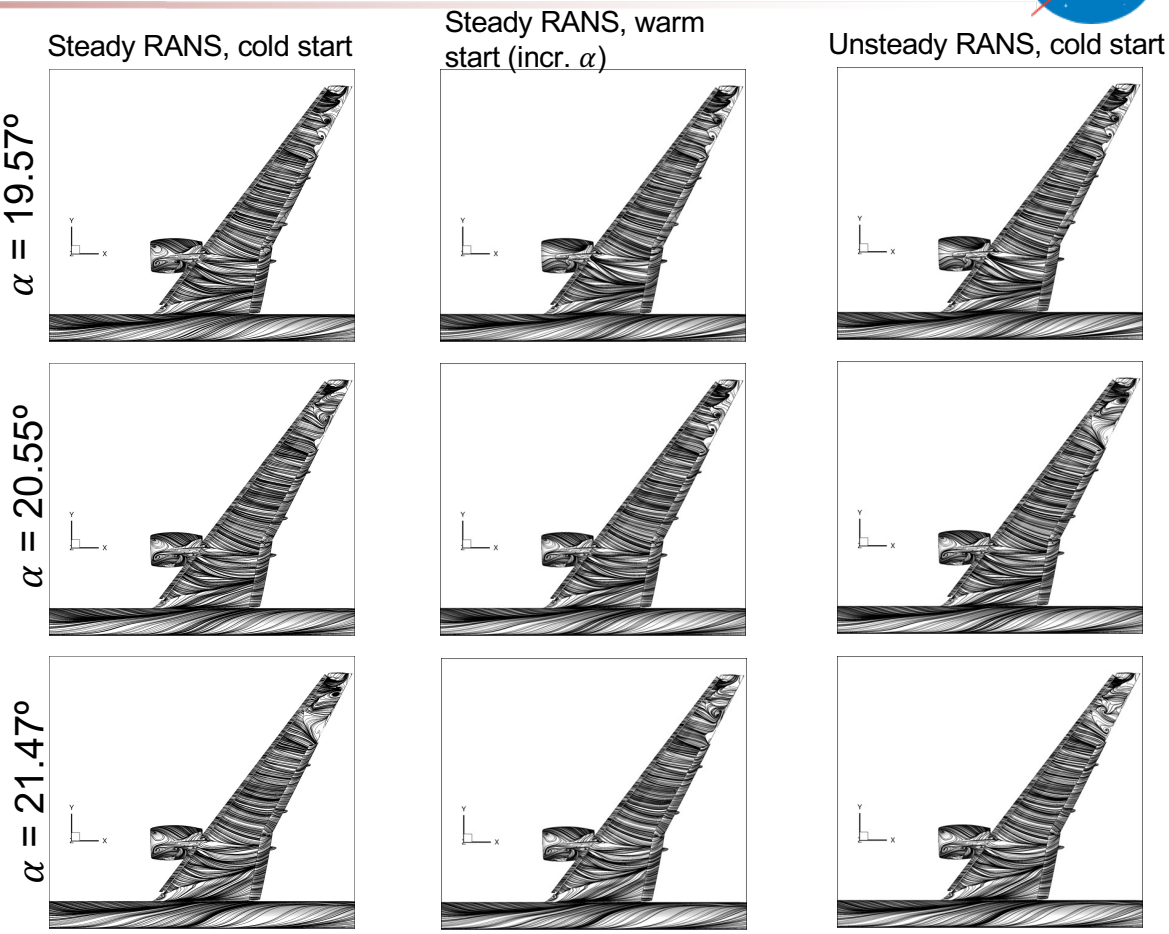
Time history and nonlinear iteration history of lift for unsteady and steady simulations, respectively, initialized from a cold start at α = 21.47º

c_{Lmax} Study: Alternative Solution Methods

- Additional simulation methods utilized in attempt to improve baseline SA predictions at high-α
  - Unsteady RANS, cold start
  - Steady RANS, warm start (increasing α)
  - Steady RANS, warm start (decreasing α)
- Benefit observed with steady RANS, warm start (increasing α), which delays spurious outboard separation



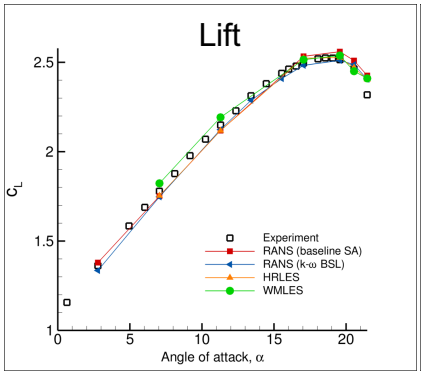


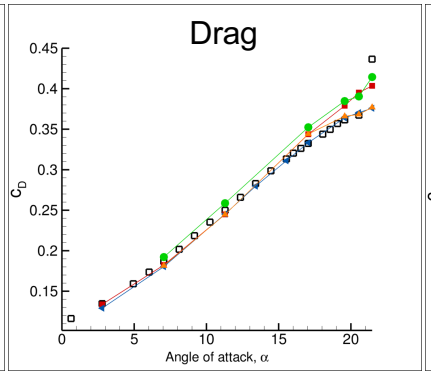


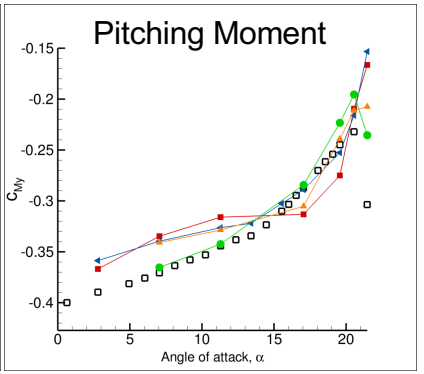
Surface streamlines for various simulation methods

c_{Lmax} Study: Comparison with Scale-Resolving Methods

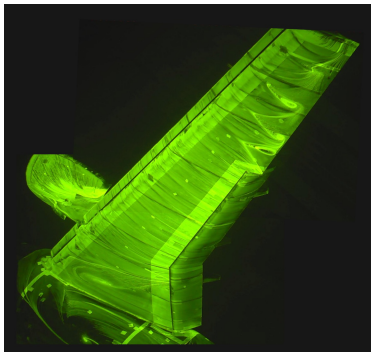
- RANS solutions compared with results from scale-resolving simulations in LAVA
  - Hybrid RANS/LES (HRLES)[1]
  - Wall-Modeled LES (WMLES)[2]
- Scale-resolving simulations also struggle to predict accurate pitch break in free air
- Validity of RANS methods in free air should not be solely based on inboard separation-induced pitch break

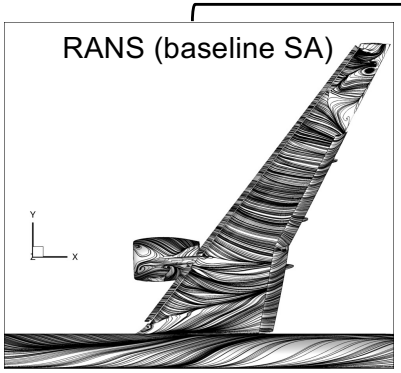


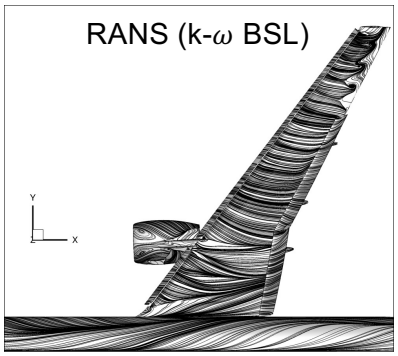


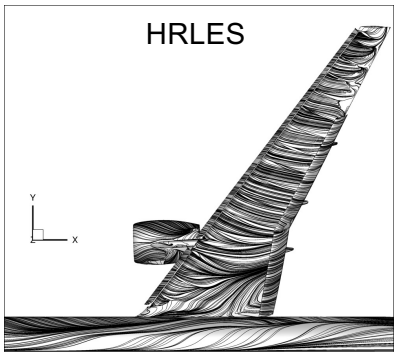


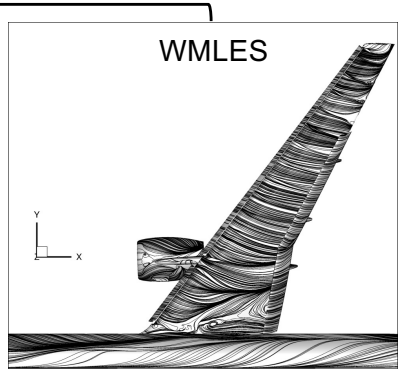
α = 21.47°







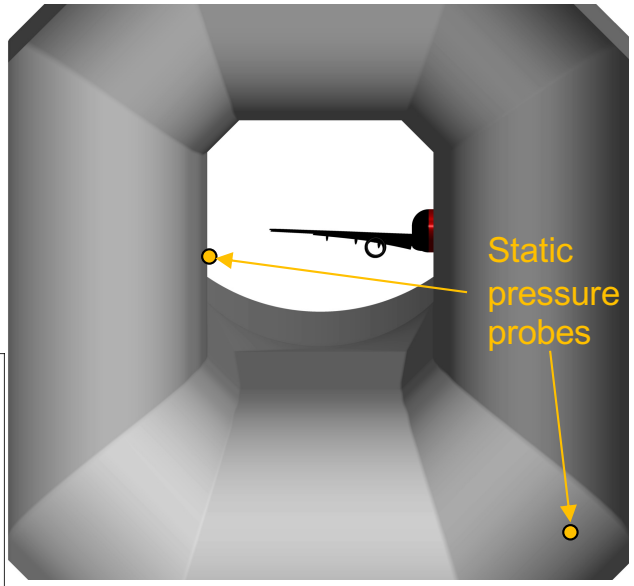


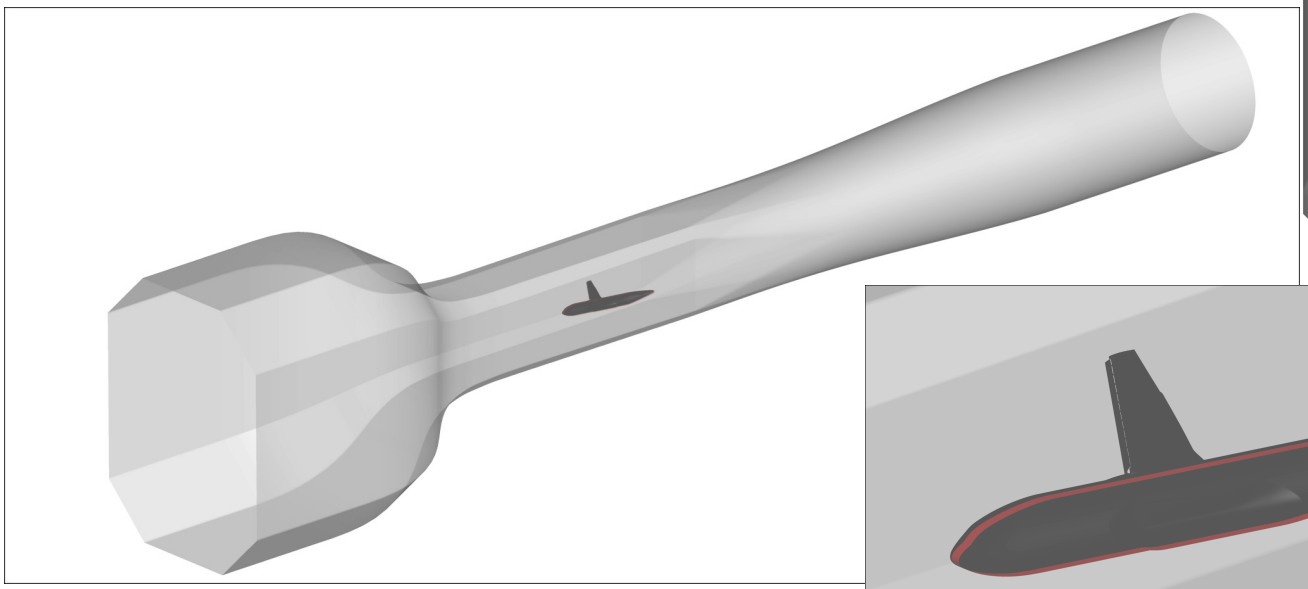


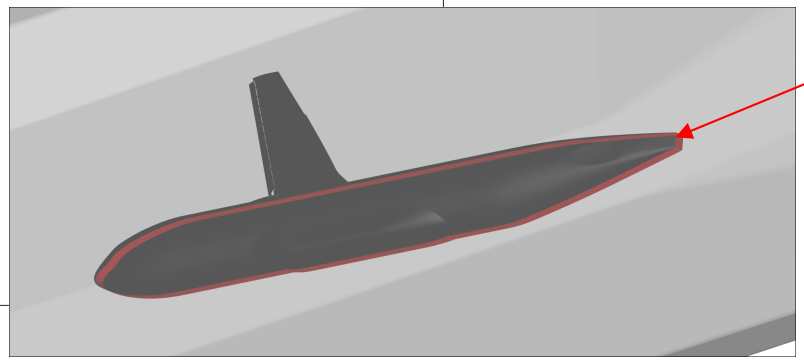
[1]Browne, O. M., Housman, J. A., Kenway, G., Ghate, A. S., and Kiris, C. C., "A Hybrid RANS-LES Perspective for the High Lift Common Research Model Using LAVA," AIAA Aviation Paper to appear , 2022.
[2]Ghate, A. S., Stich, G.-D., Kenway, G., Housman, J. A., and Kiris, C. C., "A Wall-Modeled LES Perspective for the High Lift Common Research Model Using LAVA," AIAA Aviation Paper to appear , 2022.

c_{Lmax} Study: Wind Tunnel Modeling

- QinetiQ tunnel wall interference effects studied by incorporating the CRM-HL test article
- Wind tunnel walls modeled with accompanying hardware (stand-off) used to join test article to test section wall
- Static pressure probe locations used for condition targeting indicted

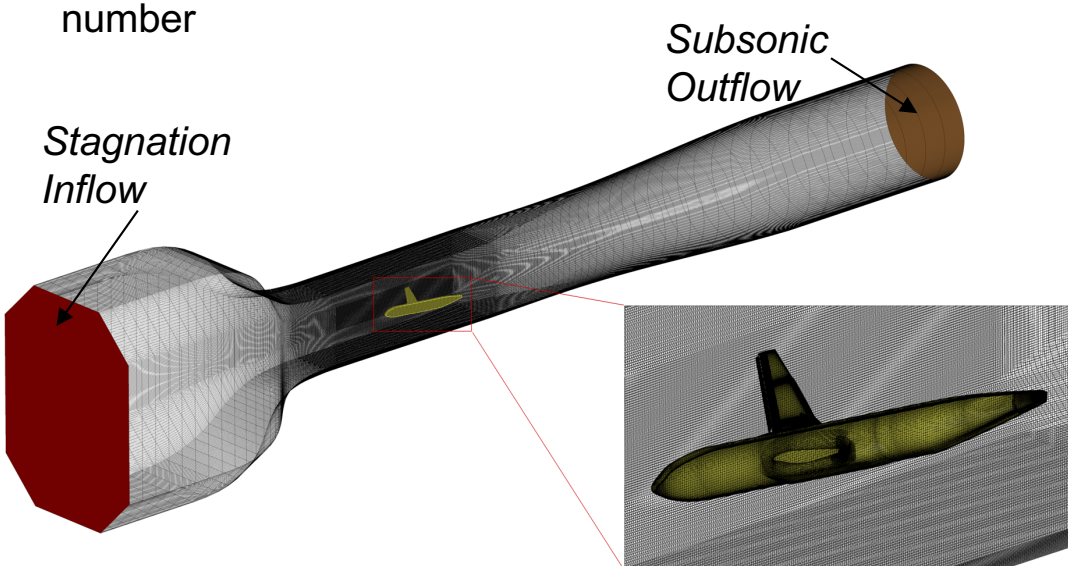


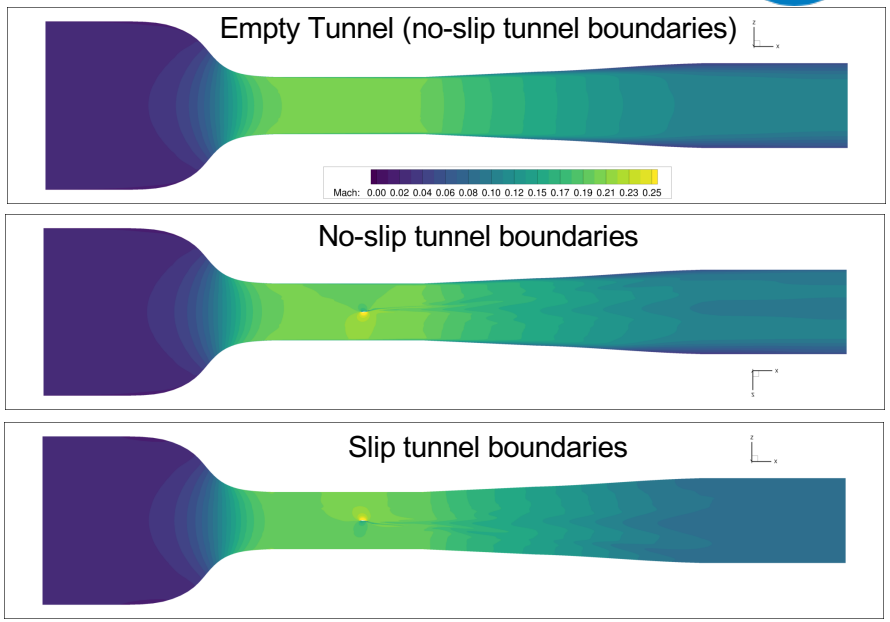




c_{Lmax} Study: Wind Tunnel Modeling

- Tunnel calibration equations that relate static pressure measurements at contraction locations to Mach number used for condition targeting
- Inviscid (slip) wall and viscous (no-slip) adiabatic wall treatments tested
- Total conditions prescribed at tunnel inflow and static pressure prescribed at outflow to set test section Mach number

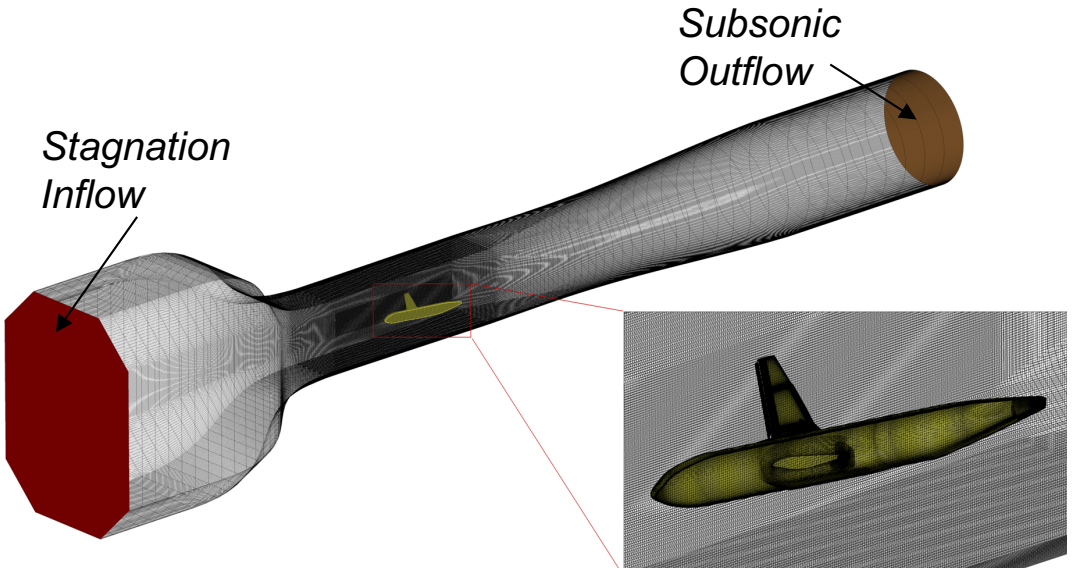


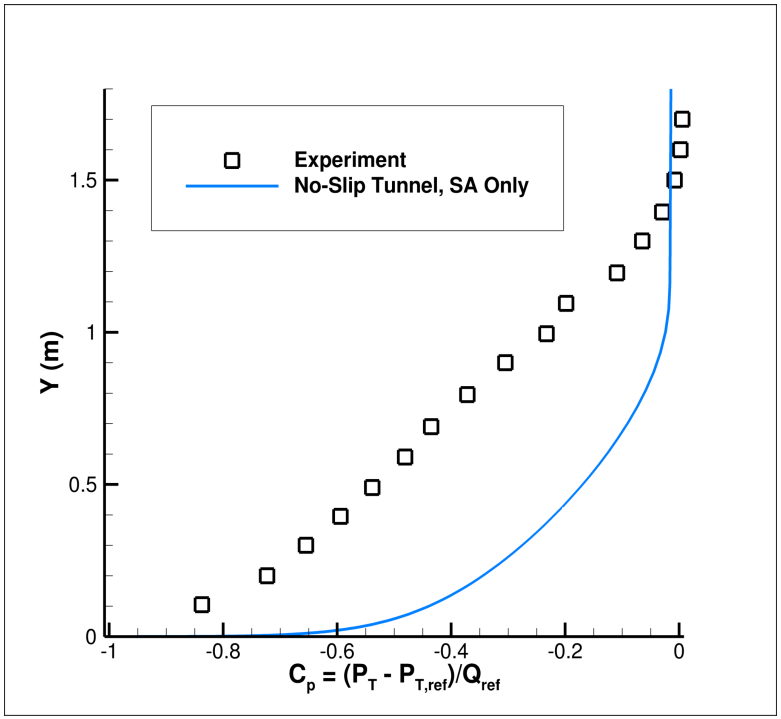


Sample Mach number distribution for in-tunnel simulations

c_{Lmax} Study: Wind Tunnel Modeling

- Condition targeting required a four step procedure
  - Initialize empty tunnel simulation with state values computed using 1-D isentropic relations
  - Solve empty tunnel simulations by iterating outflow pressure to obtain correct test section condition
  - Map empty tunnel solution to tunnel domain that includes CRM-HL
  - Solve complete tunnel + CRM-HL problem by iterating outflow pressure to obtain correct test section condition

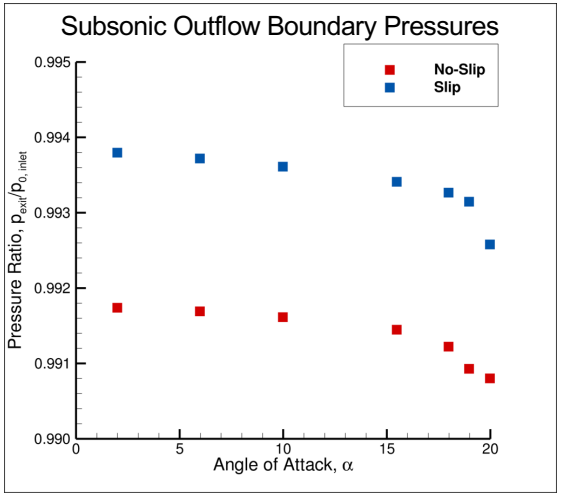


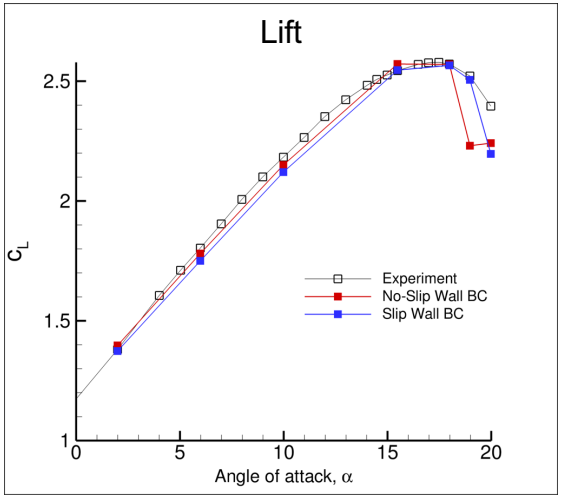


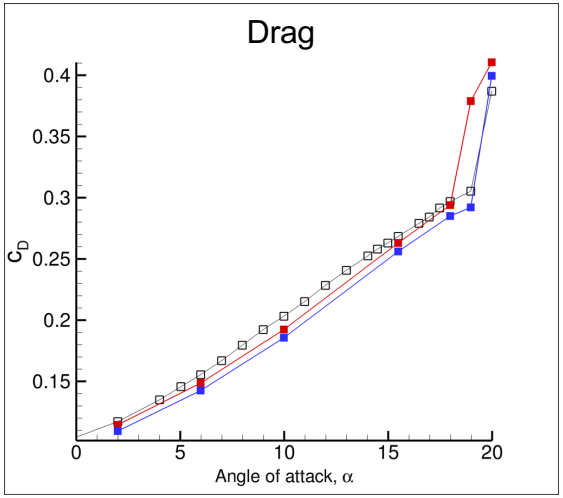
Sample Boundary Layer Profile Near Fuselage Nose (no-slip treatment)

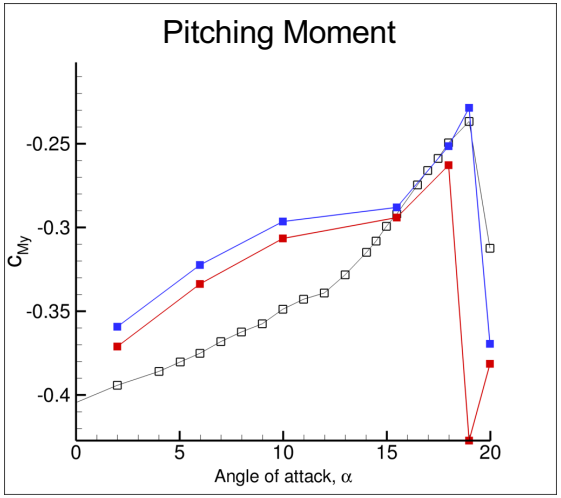
c_{Lmax} Study: Wind Tunnel Modeling

- Angle of attack sweep completed for each tunnel wall treatment
- High-α pitching moment break captured using both tunnel wall treatment methods
- Offsets in force/moment curves observed between treatments due to effective angle of attack differences
- Differences in predicted tunnel wall boundary layer relative to experiment believed to induce an early break



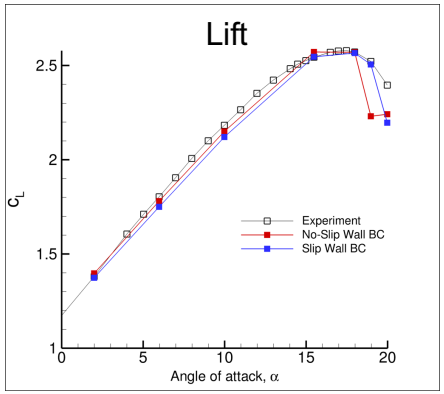


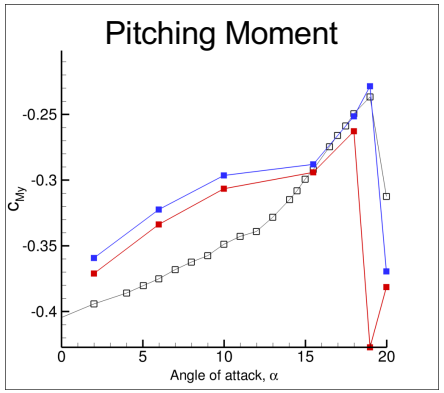


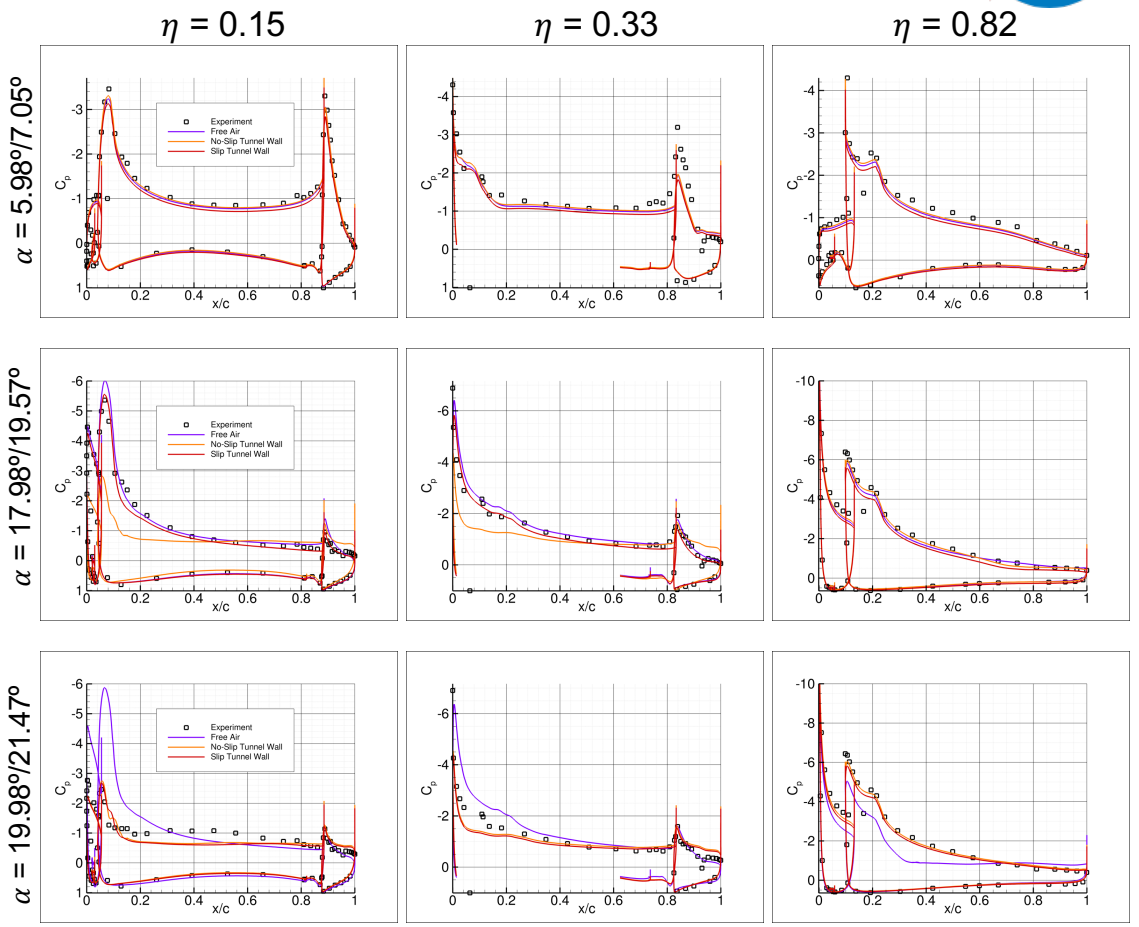


c_{Lmax} Study: Wind Tunnel Modeling

- Pressure distributions at selected angles of attack compared
  - α = 5.98º/7.05º: pressure differences on suction side related to tunnel impacts on effective angle of attack
  - α = 17.98º/19.57º: Inboard suction side pressure rise noted for no-slip tunnel treatment only
  - α = 19.98º/21.47º: Both tunnel treatments exhibit better agreement with experiment

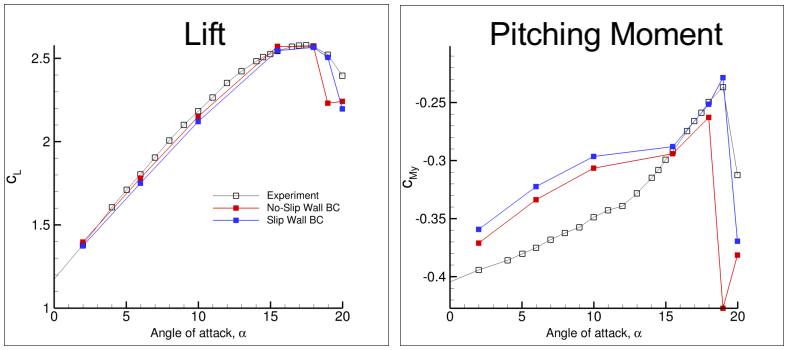


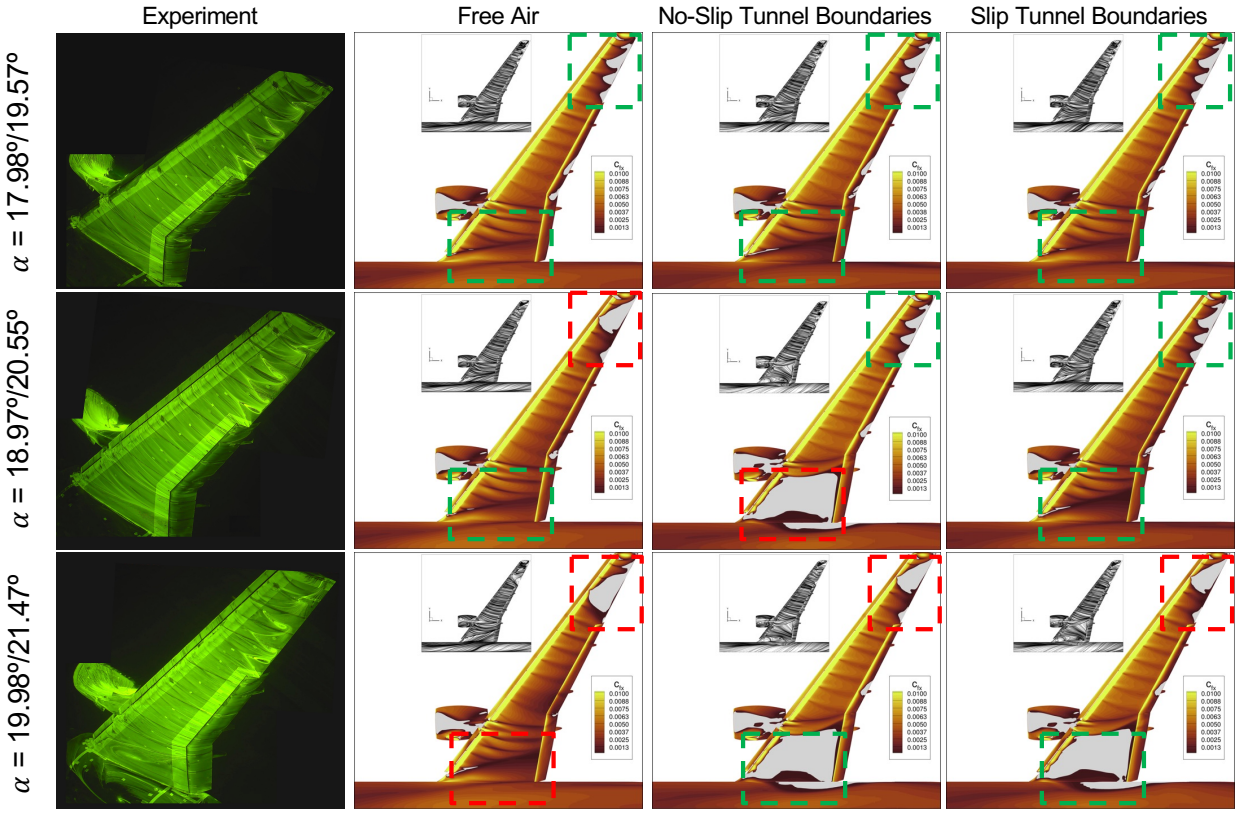




c_{Lmax} Study: Wind Tunnel Modeling

- Skin friction distributions at the highest three angles of attack used to assess separation tendencies for each simulation method
  - α = 17.98º/19.57º: All methods exhibit qualitatively similar flow topologies
  - α = 18.97º/20.55º: No-slip tunnel case exhibits premature inboard separation, free-air exhibits spurious outboard separation
  - α = 19.98º/21.47º: Both tunnel treatments experience inboard and outboard separation, inboard section in free air still attached





x-component of skin friction (C_{fx}) with surface streamlines shown in inset image

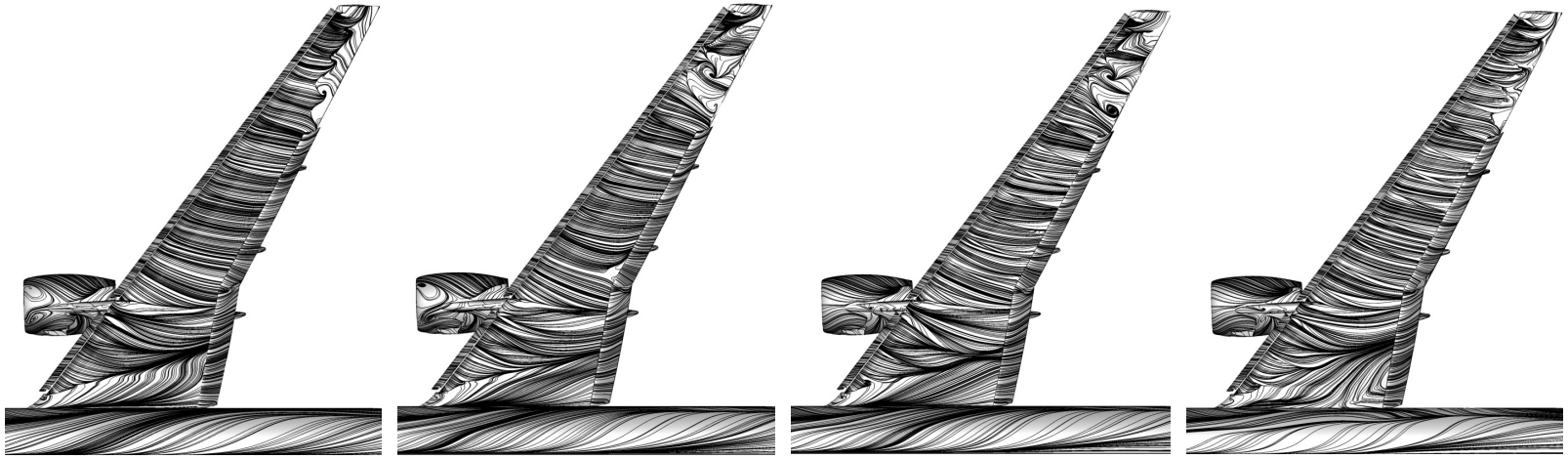
Summary of LAVA RANS Contributions to Workshop



- Solution of the PDE: Are we solving the problem correctly?
  - Steady-state convergence scrutinized for each solution
  - Mesh refinement study performed across multiple angles of attack
    - Integrated loads on mesh resolutions C and D were shown to be consistent within engineering accuracy for α = 15º
  - Unsteady analysis as well as a warm-start procedure were performed and results were consistent with steady-state integrated loads
- Sensitivity to turbulence closure: What is the most appropriate RANS model for c_{Lmax}?
  - Six turbulence model variations were studied using mesh level C
  - Low angles of attack exhibit high sensitivity in pitching moment due to flap separation differences
  - High angles of attack exhibit high sensitivity in all aerodynamic quantities due to inboard and outboard flow topology differences
  - Baseline SA model outperforms model variants with respect to c_{Lmax} prediction, but spurious outboard separation present in post-c_{Lmax} conditions
  - k-ω BSL provides best agreement with experiment, but is computationally expensive using current simulation methods and convergence criteria
- Onset of stall prediction in free air remains an unsolved challenge for all simulation methods, including scale-resolving simulation methods

Summary of LAVA RANS Contributions to Workshop

- Wind tunnel modeling provides better qualitative consistency with experiment (i.e., pitching moment break is captured), but other erroneous flow features still persist
- While all experimental flow phenomena could be predicted qualitatively using at least one method, no one RANS methodology can capture all flow topologies across entire α-range with exceptional accuracy (expected finding)
- If flow separation has a length scale on par with the MAC, the solution is very sensitive to mesh resolution, initial condition, and turbulence model choice
- With mesh refinement, there is a tendency towards larger-scale separated flow features



Steady RANS: Grid B
$\Delta s_{spanwise}$ = 0.186 m

Steady RANS: Grid D
$\Delta s_{spanwise}$ = 0.088 m

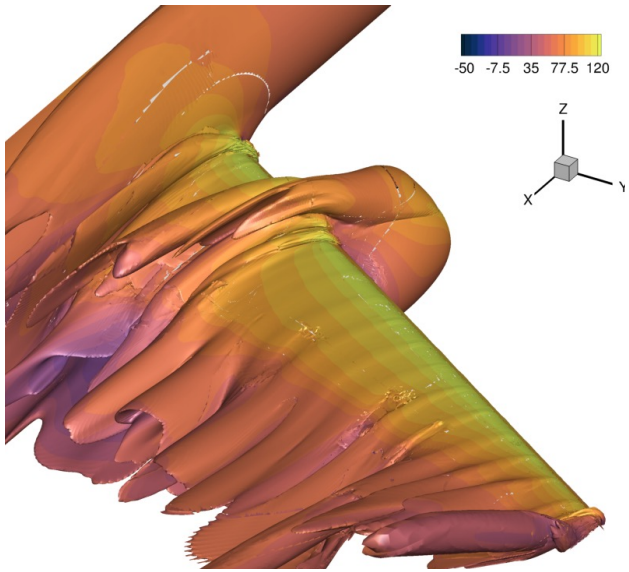
Unsteady RANS: HRLES Mesh
$\Delta s_{spanwise}$ = 0.0073
$\Delta t = 1.94\times10^{-3}$ *

HRLES: HRLES Mesh
$\Delta s_{spanwise}$ = 0.0073
$\Delta t = 1.94\times10^{-3}$

*Nondimensional time step size

Acknowledgements

- All funding was provided by the Transformational Tools and Technologies (T^3) project under NASA's Aeronautics Research Mission Directorate (ARMD)
- Computational resources provided by the NASA Advanced Supercomputing (NAS) facility at NASA Ames Research Center
- The authors would also like to acknowledge the following individuals:
  - Elisha Makarevich of Science and Technology Corp. (STC) for grid generation support
  - Christopher Rumsey, Anthony Sclafani, Niloufar Mahmoudnejad, Eric Laurendeau, and many other HLPW-4 committee organizers and participants
  - Aditya Ghate, Oliver Browne, Gaetan Kenway, Gerrit-Daniel Stich, William Chan, Jacob Wagner and many other LAVA team members for invaluable technical insight



Isosurface of vorticity magnitude flooded by x-velocity (m/s) for a sample steady RANS, free air simulation run at a near-C_{Lmax} condition.